ARMY RESEARCH LABORATORY

Evaluation of Cepstrum Algorithm with Impact Seeded Fault Data of Helicopter Oil Cooler Fan Bearings and Machine Fault Simulator Data

by Canh Ly and Andrew Bayba

ARL-TR-6344 **February 2013**

Approved for public release; distribution unlimited.

NOTICES

Disclaimers

The findings in this report are not to be construed as an official Department of the Army position unless so designated by other authorized documents.

Citation of manufacturer's or trade names does not constitute an official endorsement or approval of the use thereof.

Destroy this report when it is no longer needed. Do not return it to the originator.

Army Research Laboratory
Adelphi, MD 20783-1197

ARL-TR-6344 **February 2013**

Evaluation of Cepstrum Algorithm with Impact Seeded Fault Data of Helicopter Oil Cooler Fan Bearings and Machine Fault Simulator Data

Canh Ly and Andrew Bayba
Sensors and Electron Devices Directorate, ARL

Approved for public release; distribution unlimited.

REPORT DOCUMENTATION PAGE	Form Approved OMB No. 0704-0188

Public reporting burden for this collection of information is estimated to average 1 hour per response, including the time for reviewing instructions, searching existing data sources, gathering and maintaining the data needed, and completing and reviewing the collection information. Send comments regarding this burden estimate or any other aspect of this collection of information, including suggestions for reducing the burden, to Department of Defense, Washington Headquarters Services, Directorate for Information Operations and Reports (0704-0188), 1215 Jefferson Davis Highway, Suite 1204, Arlington, VA 22202-4302. Respondents should be aware that notwithstanding any other provision of law, no person shall be subject to any penalty for failing to comply with a collection of information if it does not display a currently valid OMB control number.
PLEASE DO NOT RETURN YOUR FORM TO THE ABOVE ADDRESS.

1. REPORT DATE *(DD-MM-YYYY)*	2. REPORT TYPE	3. DATES COVERED (From - To)
February 2013	Final	

4. TITLE AND SUBTITLE
Evaluation of Cepstrum Algorithm with Impact Seeded Fault Data of Helicopter Oil Cooler Fan Bearings and Machine Fault Simulator Data

5a. CONTRACT NUMBER

5b. GRANT NUMBER

5c. PROGRAM ELEMENT NUMBER

6. AUTHOR(S)
Canh Ly and Andrew Bayba

5d. PROJECT NUMBER

5e. TASK NUMBER

5f. WORK UNIT NUMBER

7. PERFORMING ORGANIZATION NAME(S) AND ADDRESS(ES)
U.S. Army Research Laboratory
ATTN: RDRL-SER-E
2800 Powder Mill Road
Adelphi MD 20783-1197

8. PERFORMING ORGANIZATION REPORT NUMBER
ARL-TR-6344

9. SPONSORING/MONITORING AGENCY NAME(S) AND ADDRESS(ES)

10. SPONSOR/MONITOR'S ACRONYM(S)

11. SPONSOR/MONITOR'S REPORT NUMBER(S)

12. DISTRIBUTION/AVAILABILITY STATEMENT
Approved for public release; distribution unlimited.

13. SUPPLEMENTARY NOTES

14. ABSTRACT

This report documents the evaluation of the cepstrum algorithm with seeded fault data for oil cooler fan bearings from the Impact Technologies, LLC, and Machine Fault Simulator (MFS) bearing data collected at the U.S. Army Research Laboratory (ARL). The Impact data collection was part of the Air Vehicle Diagnostic and Prognostic Improvement Program (AVDPIP), which was a three-year collaborative agreement between Impact Technologies, LLC, the Georgia Institute of Technology, and ARL. In this report, we describe the two types of data—Impact and MFS. The results of those data sets using the cepstrum algorithm are presented. It shows that under the control environment (laboratory) with not much surrounding interference, the cepstrum algorithm can clearly estimate fault frequencies such as inner race and outer race frequencies. Otherwise, the algorithm does not clearly identify other fault frequencies of rolling element bearings.

15. SUBJECT TERMS
AVDPIP, Machine Fault Simulator (MFS), oil cooler fan bearings, fault, cepstrum algorithm

16. SECURITY CLASSIFICATION OF:			17. LIMITATION OF ABSTRACT	18. NUMBER OF PAGES	19a. NAME OF RESPONSIBLE PERSON
a. REPORT	b. ABSTRACT	c. THIS PAGE			Canh Ly
Unclassified	Unclassified	Unclassified	UU	50	19b. TELEPHONE NUMBER (*Include area code*) (301) 394-0868

Standard Form 298 (Rev. 8/98)
Prescribed by ANSI Std. Z39.18

Contents

List of Figures iv

List of Tables v

1. Introduction 1

2. Kinematic Fault Frequency Calculations 1

3. Impact Seeded Fault Data Collection 2

4. ARL Machine Fault Simulator Data Collection 5

5. Cepstrum Algorithm 7

6. Results 9

7. Conclusions 13

8. References 14

Appendix A. Specifications of accelerometer, Model Vibra-metrics Model 3000 15

Appendix B. Results of Cepstrum Algorithm for MFS data 17

Appendix C. Results of the Cepstrum Algorithm for Selected Impact Data – Test 43, Bearing 2-2 27

List of Symbols, Abbreviations, and Acronyms 40

Distribution List 41

List of Figures

Figure 1. Oil-cooler bearing test-rig (photo from Impact Technologies, LLC).....3

Figure 2. Top view drawing of the test rig, showing the locations of the test cells, accelerometers, and sensors. 3

Figure 3. MFS manufactured by SpectraQuest, Inc. 6

Figure 4. Flow diagram of the cepstrum algorithm. 8

Figure 5. MFS time waveform and result using cepstrum for outer race seeded fault. 9

Figure 6. Result of cepstrum for outer race Level 5 seeded fault without gearbox and magnet load. 10

Figure 7. Impact data time waveform and plot of the resulting cepstrum. 12

Figure B-1. Ball seeded fault bearings with and without gearbox and magnet load for level 1…18

Figure B-2. Ball seeded fault bearings with and without gearbox and magnet load for level 3…19

Figure B-3. Ball seeded fault bearings with and without gearbox and magnet load for level 5…20

Figure B-4. Cepstrum algorithm for the inner race seeded fault bearings with and without gearbox and magnet load for level 1. 21

Figure B-5. Cepstrum algorithm for the inner race seeded fault bearings with and without gearbox and magnet load for level 3. 22

Figure B-6. Cepstrum algorithm for the inner race seeded fault bearings with and without gearbox and magnet load for level 5. 23

Figure B-7. Cepstrum algorithm for the outer race seeded fault bearings with and without gearbox and magnet load for level 1. 24

Figure B-8. Cepstrum algorithm for the outer race seeded fault bearings with and without gearbox and magnet load for level 3. 25

Figure B-9. Cepstrum algorithm for the outer race seeded fault bearings with and without gearbox and magnet load for level 5. 26

List of Tables

Table 1. Independent/controlled variables of planned oil cooler bearing seeded fault tests. 4
Table 2. Oil cooler bearing geometry parameters. 4
Table 3. Calculated bearing fault frequencies for 210 SFFC. 4
Table 4. ER16K bearing geometry. 6
Table 5. Calculated bearing fault frequencies for ER16K. 7
Table 6. Estimated fault frequencies and errors. 11
Table 7. ARL-MFS Test data files. 13

INTENTIONALLY LEFT BLANK.

1. Introduction

The shift towards a condition-based maintenance approach has the potential to provide a substantial benefit with regards to reliability, availability, safety, and maintainability. To apply this approach, techniques for monitoring the condition of a bearing must be put into practice. There are many potential methods, the most traditional being the use of statistical time-domain features, such as the root mean square, peak to peak, kurtosis, and crest factor (*1*). The use of the vibration spectrum and bearing fault frequencies is also common; however, in many instances, the bearing fault frequency peaks in the vibration spectrum are close to the noise floor during the incipient stages of bearing damage (*2*). One of the more popular techniques is the high frequency envelope method, also referred to as bearing envelope analysis. Demodulation of a specific high frequency band and extracting energy from the envelope spectrum at the bearing fault frequencies have shown to be more effective than monitoring the fault frequencies using the traditional fast Fourier transform (FFT) spectrum (*3*). Another approach in estimating the frequency is the cepstrum method. The cepstrum method can determine discrete fault frequencies, which provide the advantage of detecting periodicity in a frequency spectrum and accurately determining its frequency spacing. In this report, the cepstrum method is evaluated by applying it to two independent seeded fault data sets to identify the fault frequency of a bearing under controlled laboratory test environments. The resulting fault frequency is then compared to theoretical fault frequencies for the particular bearing. The data sets are Impact data for UH-60 helicopter oil cooler bearings and the U.S. Army Research Laboratory (ARL) generated data on general purpose ball bearings.

The organization of the report consists of kinematic fault frequency calculations in section 2, Impact seeded fault data collection in section 3. Section 4 describes ARL's experimental setup and the data acquired by ARL using the machine fault simulator. Section 5 presents the description of cepstrum algorithm, followed by the results in section 6. Conclusions and suggestions for future work are provided in section 7.

2. Kinematic Fault Frequency Calculations

For rolling element bearings, there are specific frequencies related to damage at a particular location on the bearing, such as the inner or outer race; these specific frequencies are called the bearing fault frequencies and are based on known kinematic relationships. The bearing fault frequency equations—ball pass frequency inner race (BPFI), the ball pass frequency outer race (BPFO), the ball spin frequency (BSF), and the fault train frequency (FTF)—are listed in equations 1–5. The parameters used to calculate the bearing fault frequencies are based on the

bearing shaft speed (f) and geometric parameters, which include the following: the number of rolling elements, N_b; the pitch diameter, P_d; the ball diameter, B_d; and the contact angle, θ.

$$BPFI = \frac{N_b}{2} * f\left[1 + \left(\frac{B_d}{P_d}\right)\cos\theta\right] \tag{1}$$

$$BPFO = \frac{N_b}{2} * f\left[1 - \left(\frac{B_d}{P_d}\right)\cos\theta\right] \tag{2}$$

$$BSF = \left(\frac{P_d}{2 * B_d}\right) * f\left[1 - \left(\left(\frac{B_d}{P_d}\right)\cos\theta\right)^2\right] \tag{3}$$

$$FTF = \frac{f}{2}\left[1 - \left(\frac{B_d}{P_d}\right)\cos\theta\right] \tag{4}$$

$$\text{Rolling Element Defect Frequency} = 2 * \text{BSF} \tag{5}$$

3. Impact Seeded Fault Data Collection

Impact Technologies, LLC, designed and built a test rig under the Army contract number W911NF-07-2-0075, shown in figure 1. The top view of the test rig is shown in figure 2, which allowed for simultaneous test runs of up to four bearings in separate test cells. These test cells were labeled Test Cell 1, Test Cell 2, Test Cell 3, and Test Cell 4.

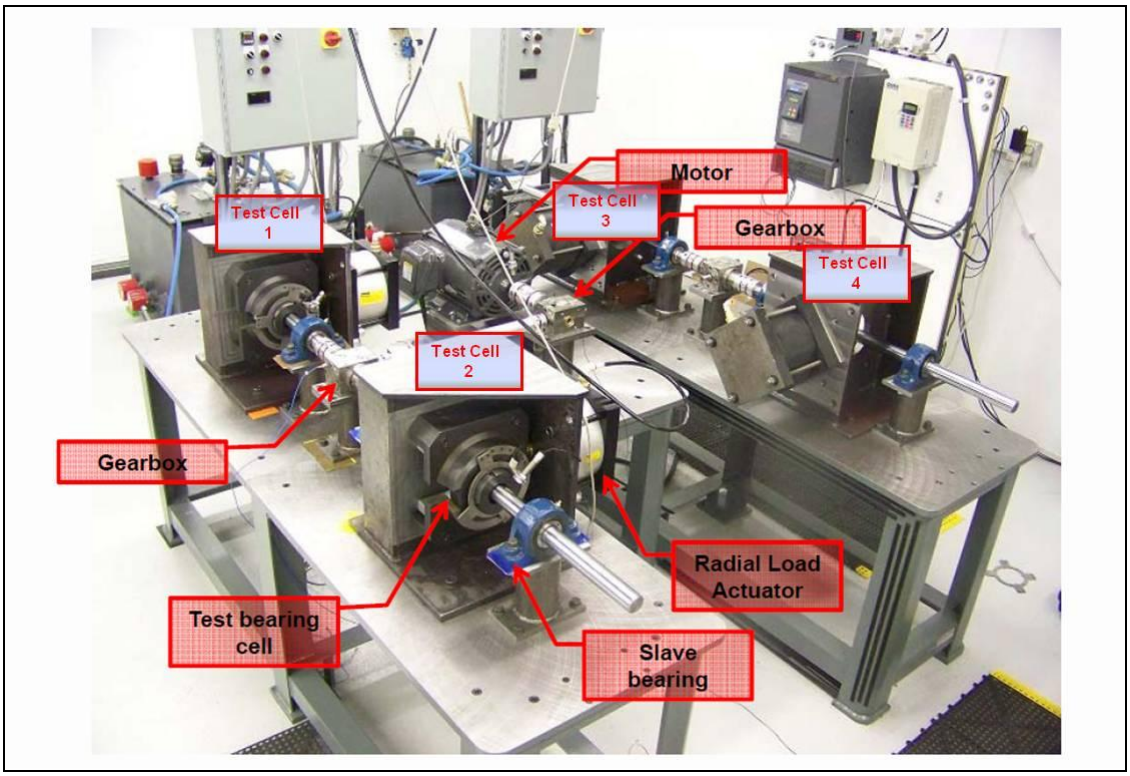

Figure 1. Oil-cooler bearing test-rig (photo from Impact Technologies, LLC).

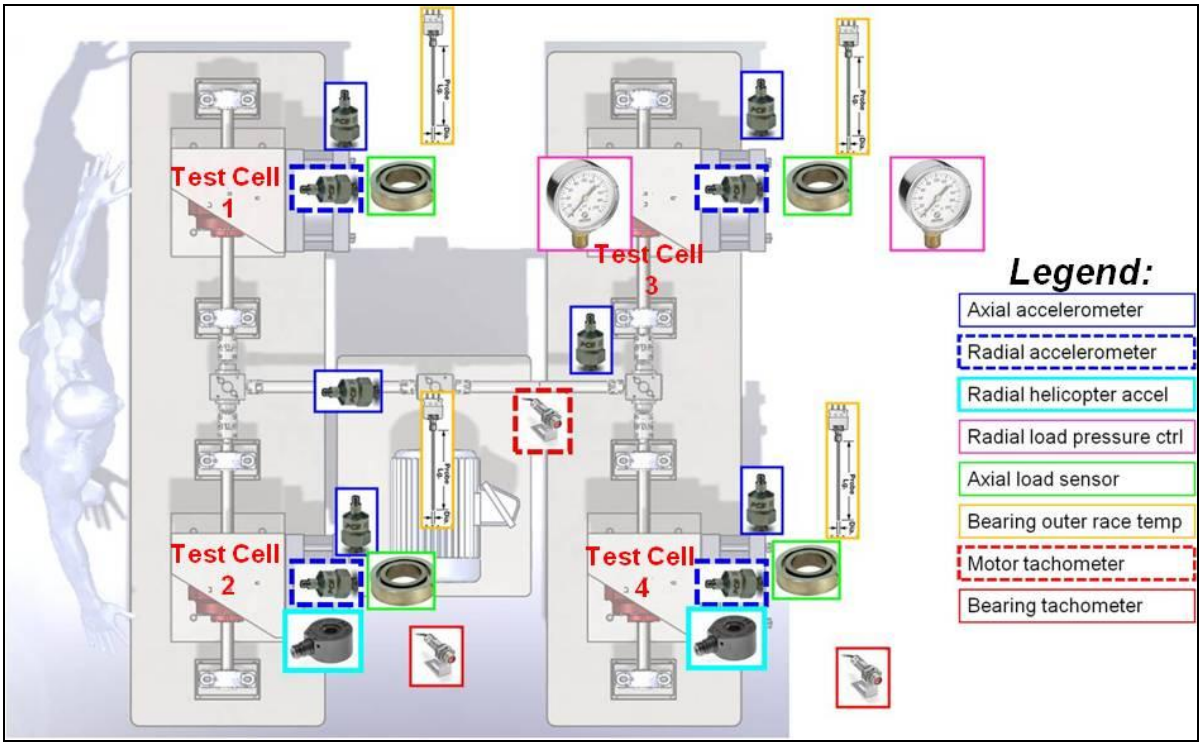

Figure 2. Top view drawing of the test rig, showing the locations of the test cells, accelerometers, and sensors.

The test rig provides the ability to perform accelerated fatigue damage progression with controlled/known conditions (independent variables), as shown in table 1.

Table 1. Independent/controlled variables of planned oil cooler bearing seeded fault tests.

Variables	Values	Notes
Bearing type	H-60 oil cooler bearings	Original Equipment Manufacturer (OEM) (MRC Company), Part No. 210SFFC
Speed	4500 RPM	Manufacture limits max speed to 4500 RPM
Load	Overload considered 3000 lb axial 5000 lb radial	The field bearings are not believed to have high loads, but we performed accelerate degradation to test multiples bearings to gain statistical relevance and extrapolate results to scale for field conditions.
Temperature	Constant	Ambient/controlled lab environment
Humidity	Ambient	Expected to have a minimal effect because of the relative short duration of the test and the constant presence/regular changing of the grease
Corrosion	Several levels: None, mild, medium, severe	The initial level of corrosion is a seeded fault. The levels are named as Corrosion Level 0 (none), 1 (mild), 2 (medium or moderate), and 3 (severe).

The geometric parameters for the oil cooler helicopter bearing used in the test rig are listed in table 2.

Table 2. Oil cooler bearing geometry parameters.

Bearing Geometry Parameters	
No. of rolling elements	10
Ball diameter (mm)	12.7
Pitch diameter (mm)	70
Contact angle	0

Using equations 1–5 described in section 2 and a shaft speed of 75 Hz, the bearing fault frequencies for the oil cooler bearings, 210 SFFC, can be calculated in a straightforward manner and are shown in table 3. The calculated fault frequencies and the ones observed in the frequency spectrum might differ by a few hertz; this is because the bearing fault frequency equations are based on the kinematic assumption of no slip, which is never perfectly achieved in a real system.

Table 3. Calculated bearing fault frequencies for 210 SFFC.

Bearing Fault Frequency Name	Frequency(Hz)
BPFI	443.04
BPFO	306.96
BSF	199.89
FTF	30.70
Roll element	399.78

Each test cell of the test rig consists of a radial and axial accelerometer, a load cell to measure the axial load, pneumatic regulators to monitor the radial load, thermocouples attached on the bearing raceways, and a tachometer signal to provide a measure of the shaft speed. Data were acquired using a National Instruments-based PXI system; the vibration data were sampled at a rate of 102.4 KHz. The signals were acquired from accelerometers mounted at different locations, shown in figure 2. Each data file consisted of 102,400 samples, which provided a sampling time of 1 s for each data file and a frequency resolution of 1 Hz for spectrum analysis.

For this report, we selected the following data files for the evaluation of the cepstrum algorithm. The filenames of these files are as follows:

```
4462-090706_161048-2_second_1_Test09.mat
4462-091221_141641_second_1_Test43.mat
4462-100113_132900_second_1_Test43.mat
4462-100113_160655_second_1_Test43.mat
4462-100114_133856_second_1_Test43.mat
4462-100118_152841_second_1_Test43.mat
4462-100121_131843_second_1_Test43.mat
4462-100121_141201_second_1_Test43.mat
4462-100125_172413_second_1_Test43.mat
4462-100121_141201_second_1_Test43.mat
4462-100125_174605_second_1_Test43.mat
4462-100125_181823_second_1_Test43.mat
```

These data files were selected from a large data set that represents a run-to-fail test. The goal is to evaluate how well the algorithm works on the data set.

For more information about the description of the tests and the name convention of the data files, refer to reference 6.

4. ARL Machine Fault Simulator Data Collection

The Machine Fault Simulator (MFS) is a test rig, shown in figure 3, operated by ARL and manufactured by SpectraQuest Inc. The rig is specifically designed for studying defects in machinery components, such as rolling element bearings, and is outfitted with mounting holes for accelerometers in positions of interest. As can be seen in the figure, the rig is a complete drive train consisting of an electric motor; shaft with weights, pulleys, and belts; a gearbox; and a magnetic load. The shaft was loaded with two 11-lb cylindrical weights, which rotate with the shaft, and was supported by two ball bearings near the ends of the shaft. The bearing closest to the motor was the bearing under test, while the bearing further from the motor was always a known good bearing. The gearbox and magnetic load could easily be disengaged from the drive

train by removal of the pulleys. Runs were performed with the gearbox and magnetic load both engaged and disengaged.

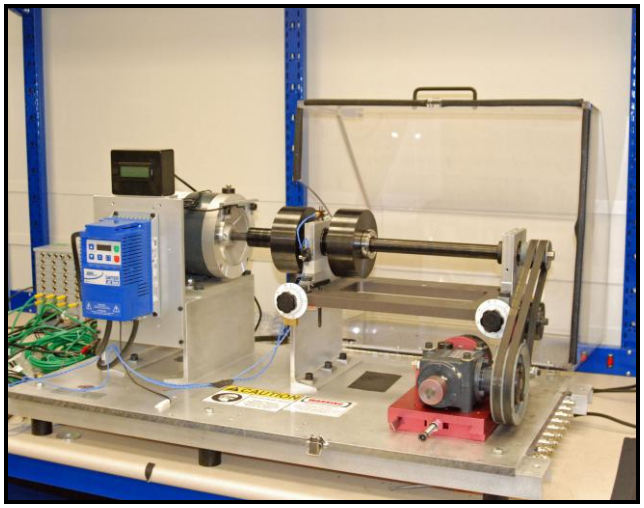

Figure 3. MFS manufactured by SpectraQuest, Inc.

For the MFS experiments, the bearings under test were Rexnord ER16K, general purpose ball bearings. All of the bearings were new and most had defects intentionally made in them (seeded faults). There were five good bearings and 15 bearings with seeded faults. The faulted bearings consisted of five bearings with ball faults, five bearings with inner race faults, and five bearings with outer race faults. The bearings of each fault type had five levels of damage of the specific defect (Levels 1–5). For this report, only levels 1, 3, and 5 were evaluated (the lowest, middle and highest levels), supposing the intermediate levels of 2 and 4 to be unnecessary for this evaluation. The bearing geometry is described in table 4.

Table 4. ER16K bearing geometry.

MFS Bearing Geometry Parameters	
No. of rolling elements	9
Ball diameter (mm)	7.937
Pitch diameter (mm)	38.5
Contact angle	0

Using equations 1–5 shown in section 2 and a shaft speed of 35 Hz, the bearing fault frequencies for the MFS-ARL bearings, Rexnord ER16K, can be calculated in a straightforward manner and are shown in table 5. The calculated fault frequencies and the ones observed in the frequency spectrum might differ by a few hertz; this is because the bearing fault frequency equations are based on the kinematic assumption of no slip, which is never perfectly achieved in a real system.

Table 5. Calculated bearing fault frequencies for ER16K.

Bearing Fault Frequency Name	Frequency(Hz)
BPFI	189.982
BPFO	125.018
BSF	81.246
FTF	13.891
Roll element	162.492

The test rig was instrumented with two tri-axial accelerometers, manufactured by Vibra-metrics, Inc. Specifications of the accelerometer are shown in appendix C.

Data were collected by a SoMat eDAQ-lite data acquisition system. The MFS system was allowed to "warm-up" for 5 min before collecting data for each bearing. For each run, five channels (signals) were recorded for a little over 10 s. The channels were the tachometer pulse, and the four accelerometer signals described earlier. The sampling rate was 100 KHz. The data, as collected, were stored in a proprietary binary format.

After all the runs, exactly 10 s of data were extracted and converted into tab delimited ASCII format for each run. The columns of the data were ordered as follows: tachometer pulse, *x*-axis (accelerometer one), *y*-axis (accelerometer one), *z*-axis (accelerometer one), and *x*-axis (accelerometer two). The extraction and conversion were performed using HBM's Infield software, version 2.3.0. For the analysis of this report, the data were processed as described damage levels 1, 3, and 5 of each of the fault types. There are three types of faults—inner race, outer race, and ball.

At each level of the damage, the data were collected with and without the gearbox box and magnetic load. Therefore, there are 18 files in total. The cepstrum algorithm was used to estimate the fault frequencies for both types of data.

5. Cepstrum Algorithm

One way of obtaining an estimate of the dominant fundamental frequency for vibration signals is to use the *cepstrum.* The cepstrum is the inverse Fourier transform of the logarithm of the magnitude of the Fourier transform of a signal (*7, 8*). Figure 4 shows the flow diagram of the cepstrum algorithm. If the log magnitude spectrum contains many regularly spaced harmonics, then the Fourier analysis of the spectrum will show a peak corresponding to the spacing between the harmonics, i.e., the fundamental frequency.

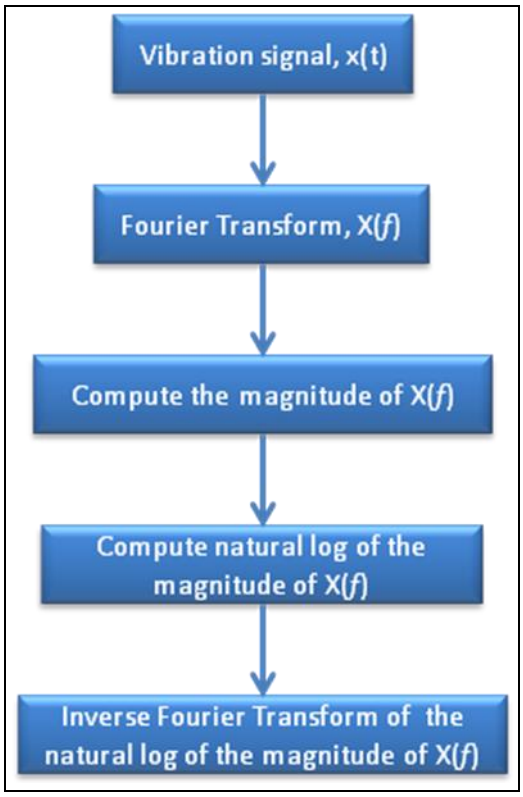

Figure 4. Flow diagram of the cepstrum algorithm.

Mathematically, the cepstral spectrum, $C(\tau)$, is calculated (*8*) as follows:

$$C(\tau) = \Im^{-1}\left\{\log\left(\left\|X(f)\right\|\right)\right\} \tag{6}$$

where $X(f) = \Im\{x(t)\}$ is the Fourier transform of $x(t)$, $\left\|X(f)\right\| = \sqrt{\left(\mathrm{Re}\{X(f)\}\right)^2 + \left(\mathrm{Im}\{X(f)\}\right)^2}$, and $\Im^{-1}\{\bullet\}$ is the inverse Fourier transform operation. $\mathrm{Re}\{\bullet\}$ is the real part and $\mathrm{Im}\{\bullet\}$ is the imaginary part of $X(f)$.

Effectively, the cepstral spectrum is considered as another signal. One can look for the periodicity in the spectrum itself. The *x*-axis of the spectrum has units of quefrency in seconds, and peaks in the spectrum (which relate to periodicities in the spectrum) are called rahmonics.

Let C_i (where i = 1, 2, ..., N) be the rahmonics of the cepstral spectrum. The fault frequency, f_{est}, from the spectrum can be estimated as follows:

$$f_{est} = \frac{1}{N-1}\sum_{i=1}^{N-1} f_i = \frac{1}{N-1}\sum_{i=1}^{N-1}\frac{1}{C_{i+1} - C_i} \tag{7}$$

6. Results

This section presents the results of the cepstrum for the MFS and Impact data. Figure 5 shows the time waveform of the bearing with the outer race seeded fault level 5 (top panel) and the result of the cepstrum (bottom panel). The bearing was tested without gearbox and magnet load. From the cepstral spectrum, magnitude (dB) vs. quefrency (s), the red vertical lines are repeated quefrency lines. The boxes indicate the coordinates of the rahmonics. Figure 6 shows just the result of the cepstrum without boxes so that one can see that the rahmonics are lined up with the theoretical values. Using equation 7, the estimated fault frequency is calculated as follows

$$f_{est}\big|_{outerrace} = \frac{1}{25}\sum_{i=1}^{25} f_i = \frac{1}{25}\sum_{i=1}^{25}\frac{1}{C_{i+1}-C_i} = 125.1196\ Hz$$

where C_i (where i = 1, 2, ... , 25) are the x-coordinates of those boxes. Since the theoretical outer race fault frequency is 125.018 Hz (from table 5), the percentage error is

$$\%\ error = \frac{\left|f_{theoretical} - f_{est}\right|}{f_{theoretical}} = \frac{\left|125.018 - 125.1196\right|}{125.018} = 0.0813\,\%$$

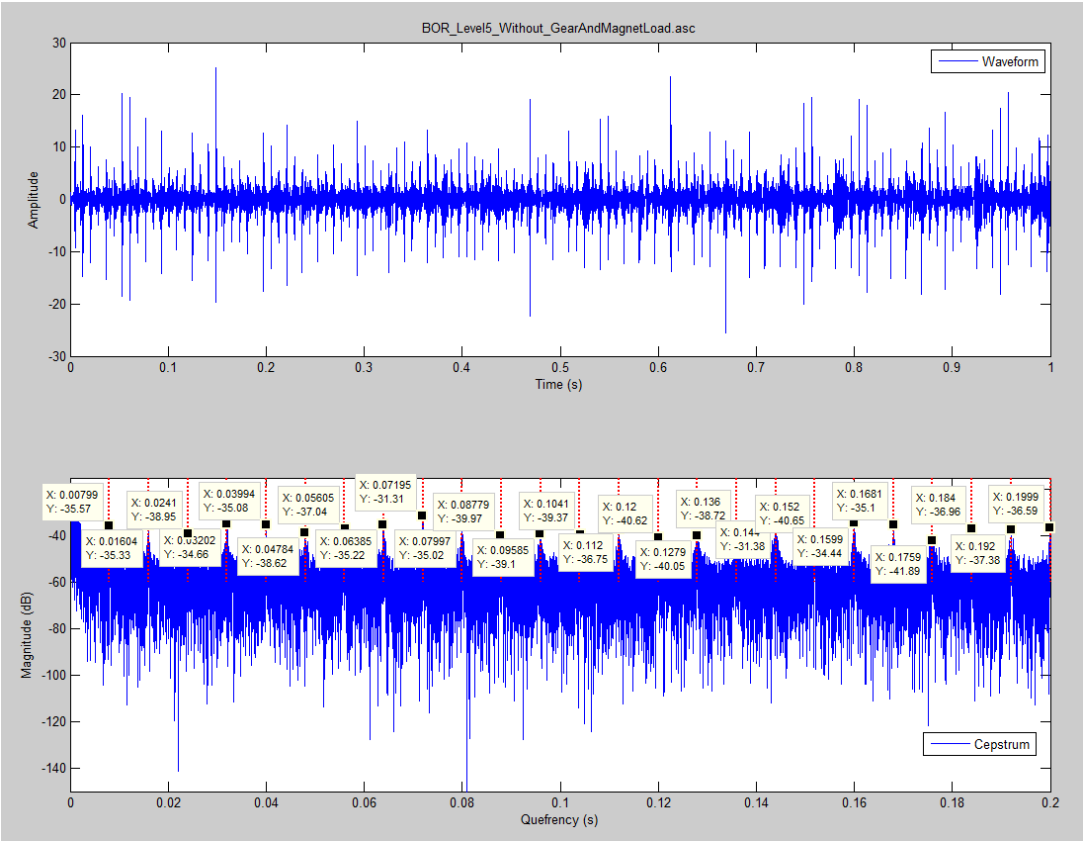

Figure 5. MFS time waveform and result using cepstrum for outer race seeded fault.

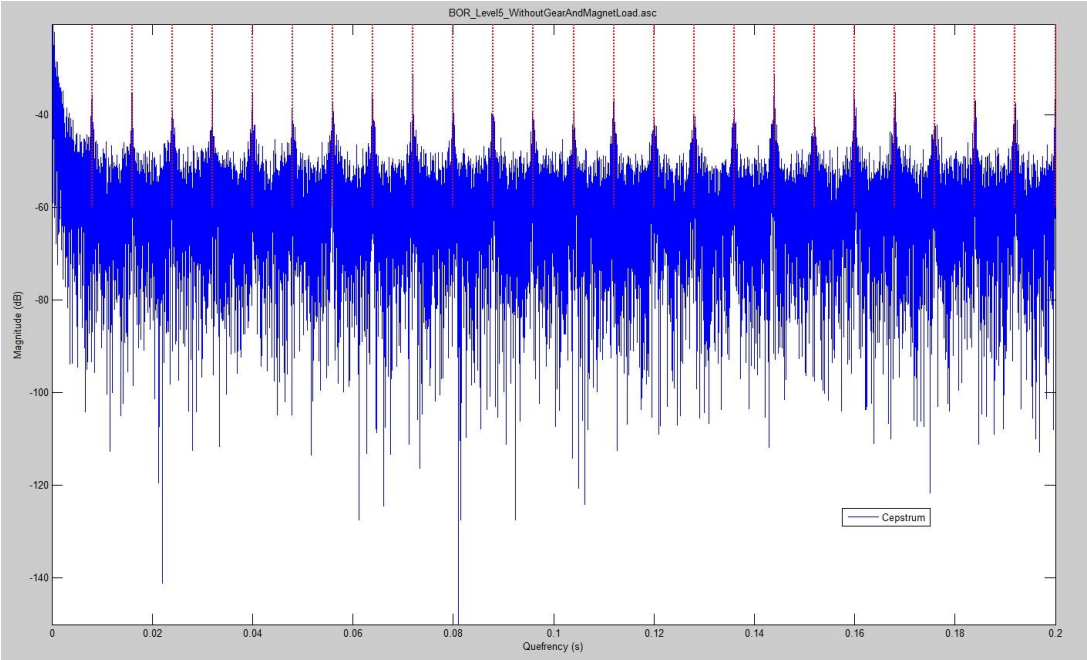

Figure 6. Result of cepstrum for outer race Level 5 seeded fault without gearbox and magnet load.

Note the fault frequency and error were calculated with a 0.2-s window. If we expand the cepstral spectrum, we will increase the numbers of rahmonics, *N*. The error will become smaller as the number of rahmonics increases because the estimated frequency gets closer to the theoretical value. Of course, the error will be smaller if the window extended from 0.2 to 1 s. However, to demonstrate how the procedure works, we chose a small window size in which all estimated frequencies shown in the window for the average estimated fault frequency calculation.

Similarly, the errors for levels 3 and 5 of the inner race and outer race fault were calculated using the same procedure as described above. Note that, for the inner race calculations, the same time window of 0.2 s produced a greater number of peaks, rahmonics, than the corresponding cepstral spectrum of the outer race. This is due to the higher frequency of the inner race fault, and thus a smaller time interval between the peaks. Table 6 shows the estimated frequencies and corresponded errors for the outer race fault and the inner race fault bearings at levels 3 and 5, with and without gearbox and magnet load engaged. For level 1, the cepstrum algorithm did not resolve either inner or outer race fault frequencies.

Table 6. Estimated fault frequencies and errors.

Bearing Fault	**Level of Severity**	**F_est (Hz) (*Without* Gearbox and Magnet Load)**	**Error (%)**	**F_est (Hz) (*With* Gearbox and Magnet Load)**	**Error (%)**
Outer race	Level 5	125.1196	0.0813	125.4252	0.3257
	Level 3	125.3714	0.2827	125.2285	0.1684
	Level 1	Not resolved	–	Not resolved	–
Inner race	Level 5	191.1164	0.60371	191.4350	0.7714
	Level 3	191.2101	0.6530	192.3857	1.2719
	Level 1	Not resolved	–	Not resolved	–

From table 6, we see clearly that the percentage error was higher when the bearing was tested with the gearbox and magnet load for both the inner and outer race cases. This is almost certainly due to additional noise from the system, since the gearbox and pulleys are known to produce significant vibrations. The error in frequency estimation of all of the inner race cases was much higher than that of the outer race cases, likely due to the losses in energy of impulses transmitted from the inner race through the balls, cage, and outer race to the accelerometer.

For the Impact data, the cepstrum algorithm was not able to resolve the fault frequency of the inner race spall. Figure 7 shows an example of the cepstrum output. There was no indication of the repeated peaks. Therefore, it was not possible to determine the frequency interval from the cepstrum using equation 7.

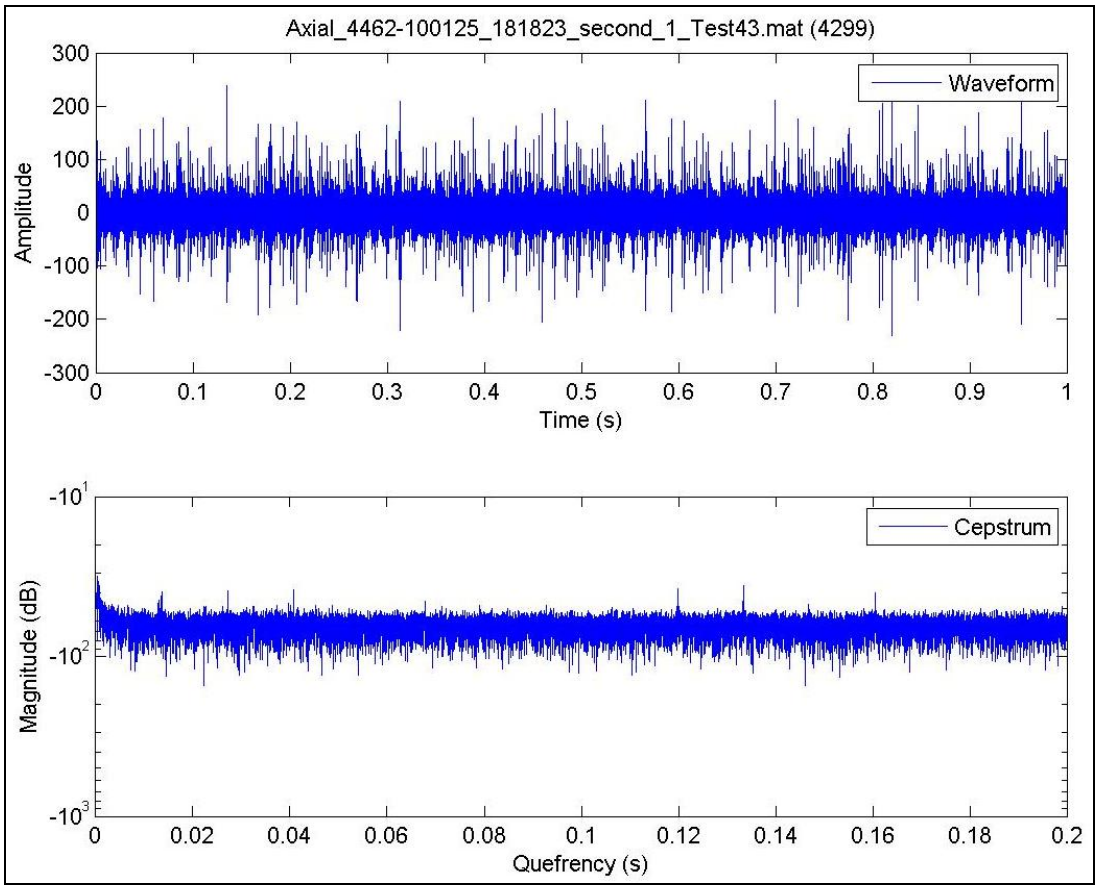

Figure 7. Impact data time waveform and plot of the resulting cepstrum.

Appendix A contains results of the cepstrum algorithm for MFS data. These test data files are summarized in table 7. There are 18 graphs—6 for ball fault, 6 for inner race fault, and 6 for outer race fault bearing data. Each fault level consists of runs/data with and without the gearbox and magnet load engaged. From the results, we see that the cepstrum algorithm only resolved the inner race and outer race fault frequencies of MFS data for level 3 and level 5 both with and without the gearbox magnet load. The algorithm could not resolve the ball fault frequency for all three levels as well as for the level 1 of the inner race and outer race faults. It was observed that the amplitude of the inner race and outer race data at for level 1 faults was much smaller than at other levels.

Table 7. ARL-MFS Test data files.

Bearing Fault	Level of Severity	Test Data Title (*With* Gearbox and Magnet Load)	Test Data Title (*Without* Gearbox and Magnet Load)
Ball	Level 5	Ball_Level5_WithGearAndMagnetLoad.asc	Ball_Level5_WithoutGearAndMagnetLoad.asc
	Level 3	Ball_Level3_WithGearAndMagnetLoad.asc	Ball_Level3_WithoutGearAndMagnetLoad.asc
	Level 1	Ball_Level1_WithGearAndMagnetLoad.asc	Ball_Level1_WithoutGearAndMagnetLoad.asc
Inner race	Level 5	BIR_Level5_WithGearAndMagnetLoad.asc	BIR_Level5_WithoutGearAndMagnetLoad.asc
	Level 3	BIR_Level3_WithGearAndMagnetLoad.asc	BIR_Level3_WithoutGearAndMagnetLoad.asc
	Level 1	BIR_Level1_WithGearAndMagnetLoad.asc	BIR_Level1_WithoutGearAndMagnetLoad.asc
Outer race	Level 5	BOR_Level5_WithGearAndMagnetLoad.asc	BOR_Level5_WithoutGearAndMagnetLoad.asc
	Level 3	BOR_Level3_WithGearAndMagnetLoad.asc	BOR_Level3_WithoutGearAndMagnetLoad.asc
	Level 1	BOR_Level1_WithGearAndMagnetLoad.asc	BOR_Level1_WithoutGearAndMagnetLoad.asc

Appendix B consists of results of the cepstrum algorithm for Impact Technologies seeded fault bearing data. The data files were selected from Test 43, Bearing 2-2, which led to an inner race spall according to the test log provided by Impact Technologies. From the broadband root-mean-square calculation, the data files were selected to represent the degradation trend as the test progressed in time. There are 24 graphs that show the results of the cepstrum algorithm in this appendix, 12 of them for the axial direction and 12 for the radial direction. From the graphs, we see that the cepstrum algorithm could not resolve the inner race fault frequency. Two possible explanations for this phenomenon are (1) the algorithm could not separate the distinct frequency from the fault that was considered as the combination of the inner race fault frequency and other fault frequencies, and (2) the signal-to-noise ratio (SNR) of this data set was not high enough.

7. Conclusions

This report presented the evaluation of the cepstrum algorithm for two independent sets of data—ARL MFS seeded fault data and Impact Technologies seeded fault data. The finding reveals that the algorithm identified the inner race and outer race fault frequencies for the MFS data at damage levels 3 and 5, but not level 1. The algorithm could not resolve the inner race fault frequency of the selected Impact Technologies data set.

From this report, we see that the cepstrum algorithm performed well with some of the data set. It clearly identified the ball bearing frequencies with a very small error. However, it failed to resolve other fault frequencies because their corresponding data have smaller SNR. The algorithm requires a high SNR to resolve the fault frequency as seen in the ARL MFS data at levels 3 and 5. Therefore, it is certainly not to be used as a single health monitoring indicator. It can be used as an indicator in conjunction with other techniques such as time statistics, frequency estimation to improve the fault frequency detection. For future investigations, one can further explore the performance of the cepstrum algorithm with a narrowband filter on the data, the deviation of the repetition frequency from the common multiple factor of the sampling frequency, and the effect of the noise level on the data.

8. References

1. Kim, E. Y.; Tan, A.C.C.; Yang, B. S.; Kosse, V. Experimental Study on Condition Monitoring of Low Speed Bearings: Time Domain Analysis. *Proceedings of the 5th Australasian Congress on Applied Mechanics, ACAM 2007*, 2007.
2. Qui, Hai; Luo, H.; Eklund, N. *On-Board Bearing Prognostics In Aircraft Engine: Enveloping Analysis or FFT*; AFRL-RX-WP-TP-2009-4141; 2009.
3. McFadden, P. D.; Smith, J. D. Vibration Monitoring of Rolling Element Bearings by High Frequency Resonance Technique – A Review. *Tribology International* **1984**, *77*, 3–10.
4. Impact's 1st Quarter Report, December 20, 2007 from Impact Technologies, LLC under the contract number W911NF-07-2-0075.
5. Impact's Final Report for Option Phase II, September 10, 2010, from Impact Technologies, LLC., under the contract number W911NF-07-2-0075.
6. Ly, C. *Impact Seeded Fault Data of Helicopter Oil Cooler Fan Bearings*; ARL-TN-0463; U.S. Army Research Laboratory: Adelphi, MD, November 2011.
7. Curtis Roads (February 27, 1996). *The Computer Music Tutorial*; MIT Press. ISBN 978-0-262-68082-0.
8. Proakis, John G.; Manolakis, Dimitris G. *Digital Signal Processing*; Pearson Prentice Hall. ISBN 978-0-13-187374-2, 2007.

Appendix A. Specifications of accelerometer, Model Vibra-metrics Model 3000

Sensitivity	±5% 10 mV/g, 1.02 mV /(m/s2) at 100 Hz
Frequency Range	• ±5% 3 Hz, 7 kHz • ±10% 2 Hz, 8 kHz • ±3 dB 1 Hz, 10 kHz
Turn-on Time	<5 s (2% of final bias)
Amplitude Range	±500 g at 72 °F
Mounted Resonance	>25 kHz
Transverse Sensitivity	<5%
Electrical Noise (typical): Output Impedance Isolation Noise Rejection Bias Volts (nominal) Power Requirements Current Regulating Diode	 Broadband 2.5 Hz to 25 kHz 1500 µg (rms) • Spectral 10 Hz 100 µg/√Hz • 100 Hz 25 µg/√Hz • 1000 Hz 10 µg/√Hz 1000 Ω >100 Meg Ω (EMI/RFI) >52 dB 7 VDC 15–30 VDC 1–6 mA
Environmental: Temperature Range	–40 to 250 °F/–40 to 121 °C
Environmental: Base Strain	<.005 g peak/µstrain
Environmental: Shock Limit	5000 g
Physical Dimensions	0.8 in h x 0.8 in w x 1.05 in d (2 cm x 2 cm x 2.7 cm)
Weight	0.35 oz/10 g
Case Material	Titanium
Mounting	10-32 removable stud
Mounting Torque	20 in-lb (2.2 N-m)
Connector	Side 4-pin

INTENTIONALLY LEFT BLANK.

Appendix B. Results of Cepstrum Algorithm for MFS data

This section shows the results of the cepstrum algorithm for MFS data—ball seeded fault bearings, inner race seeded fault bearings, and outer race seeded fault bearings.

1. Results of ball seeded fault bearings with and without gearbox and magnet load for three levels 1 (figure B-1), 3 (figure B-2), and 5 (figure B-3).
2. Results of the cepstrum algorithm for the inner race seeded fault bearings with and without gearbox magnet for three levels 1 (figure B-4), 3 (figure B-5), and 5 (figure B-6).
3. Results of the cepstrum algorithm for the outer race seeded fault bearings with and without gearbox magnet for three levels 1 (figure B-7), 3 (figure B-8), and 5 (figure B-9).

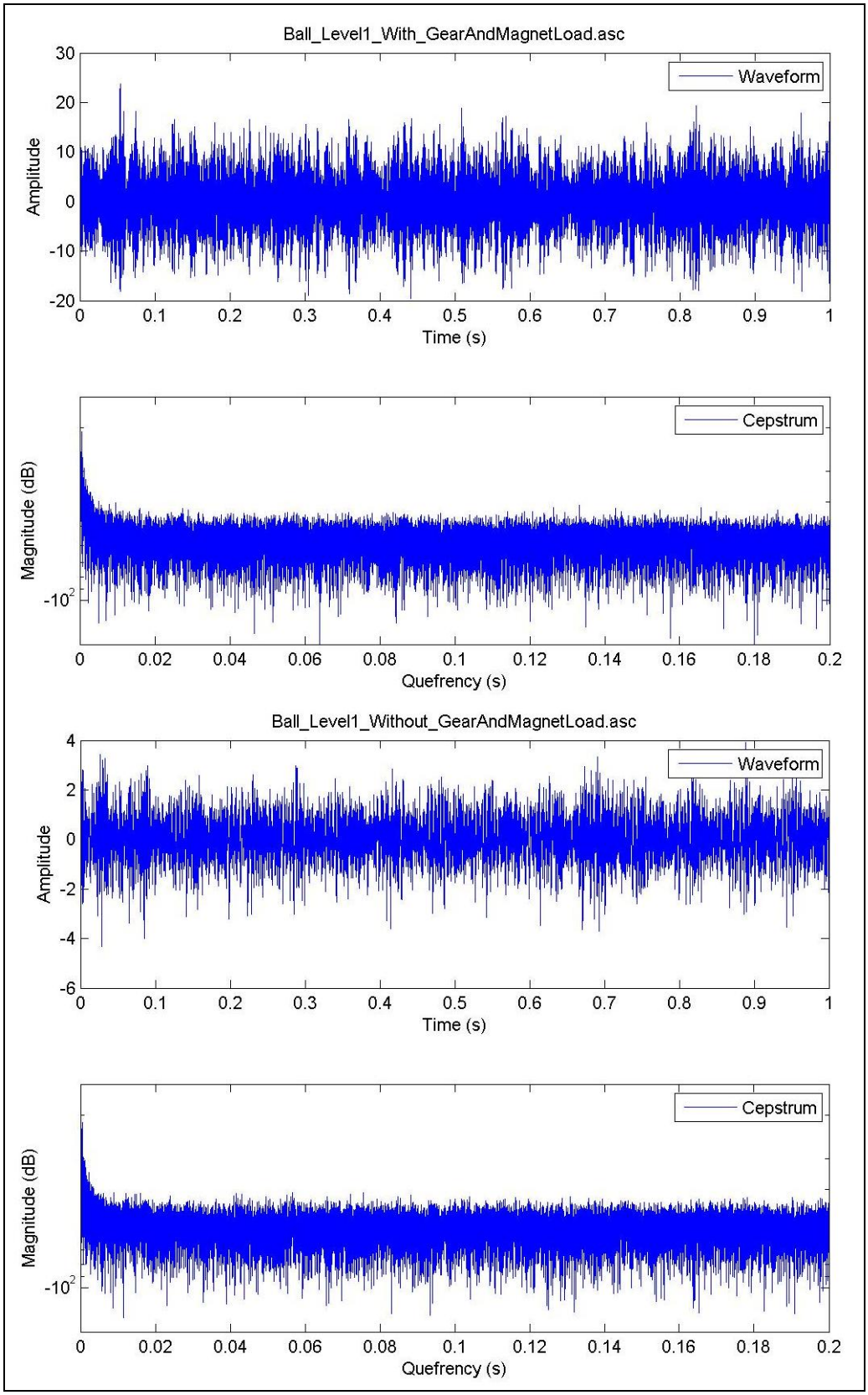

Figure B-1. Ball seeded fault bearings with and without gearbox and magnet load for level 1.

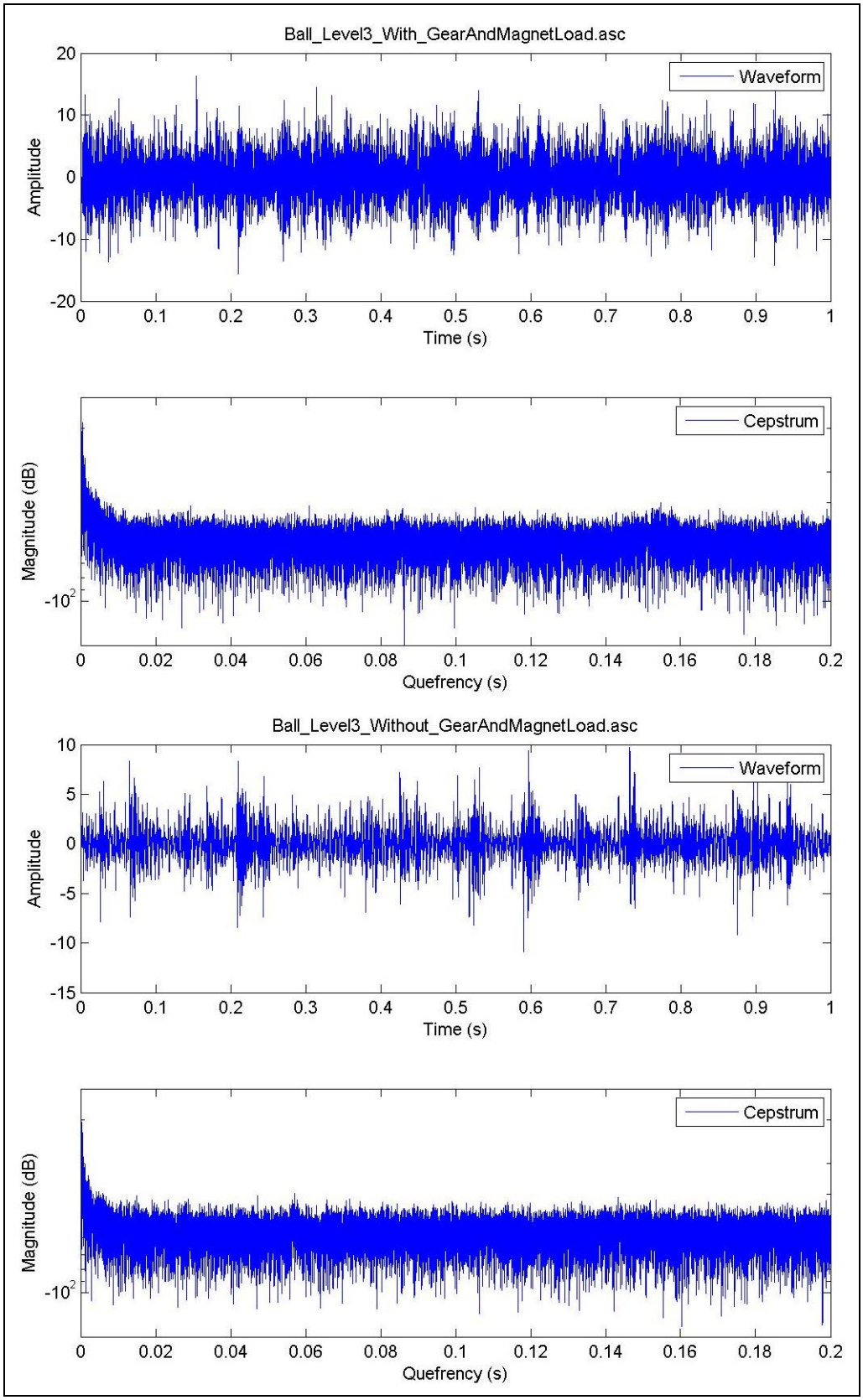

Figure B-2. Ball seeded fault bearings with and without gearbox and magnet load for level 3.

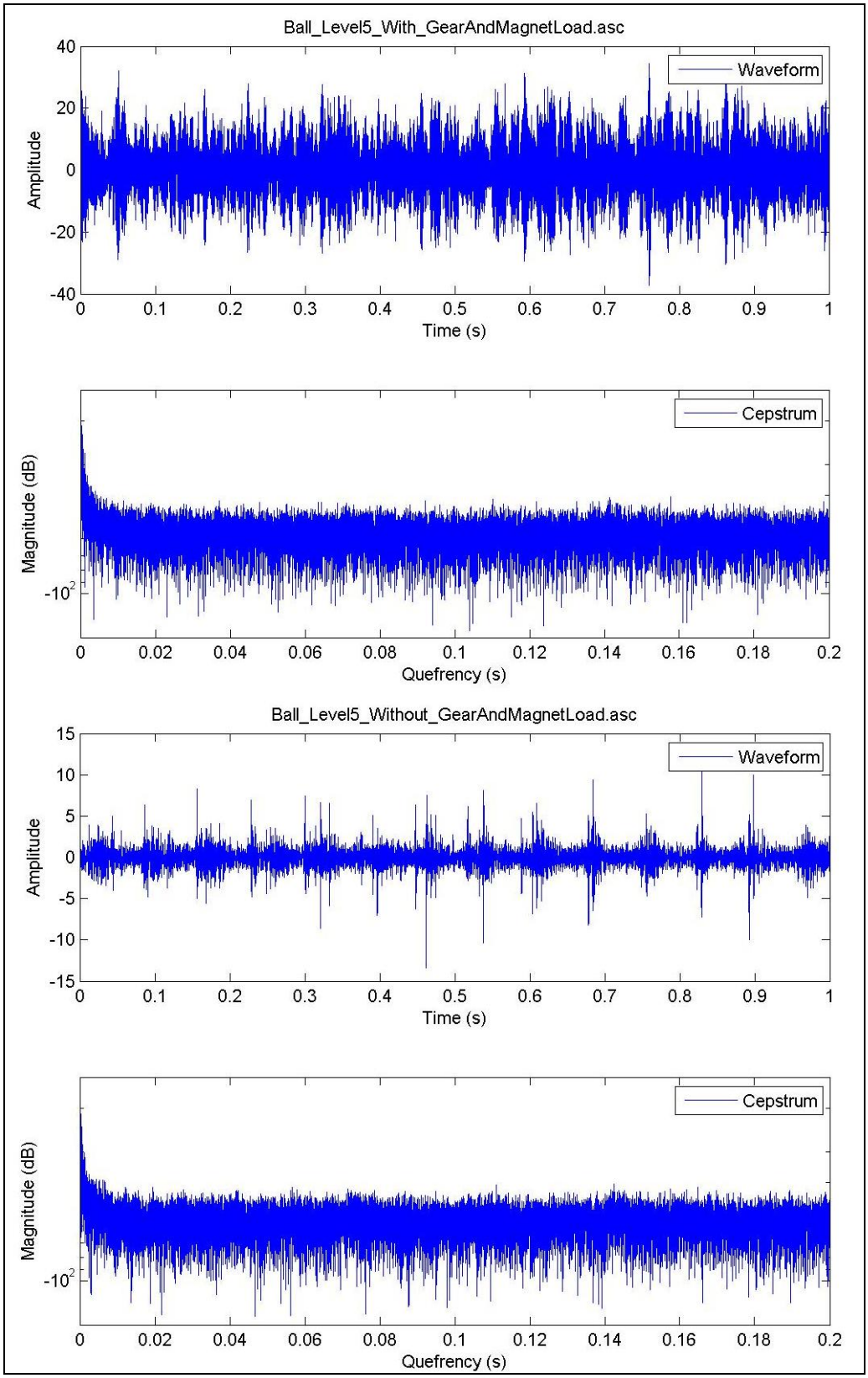

Figure B-3. Ball seeded fault bearings with and without gearbox and magnet load for level 5.

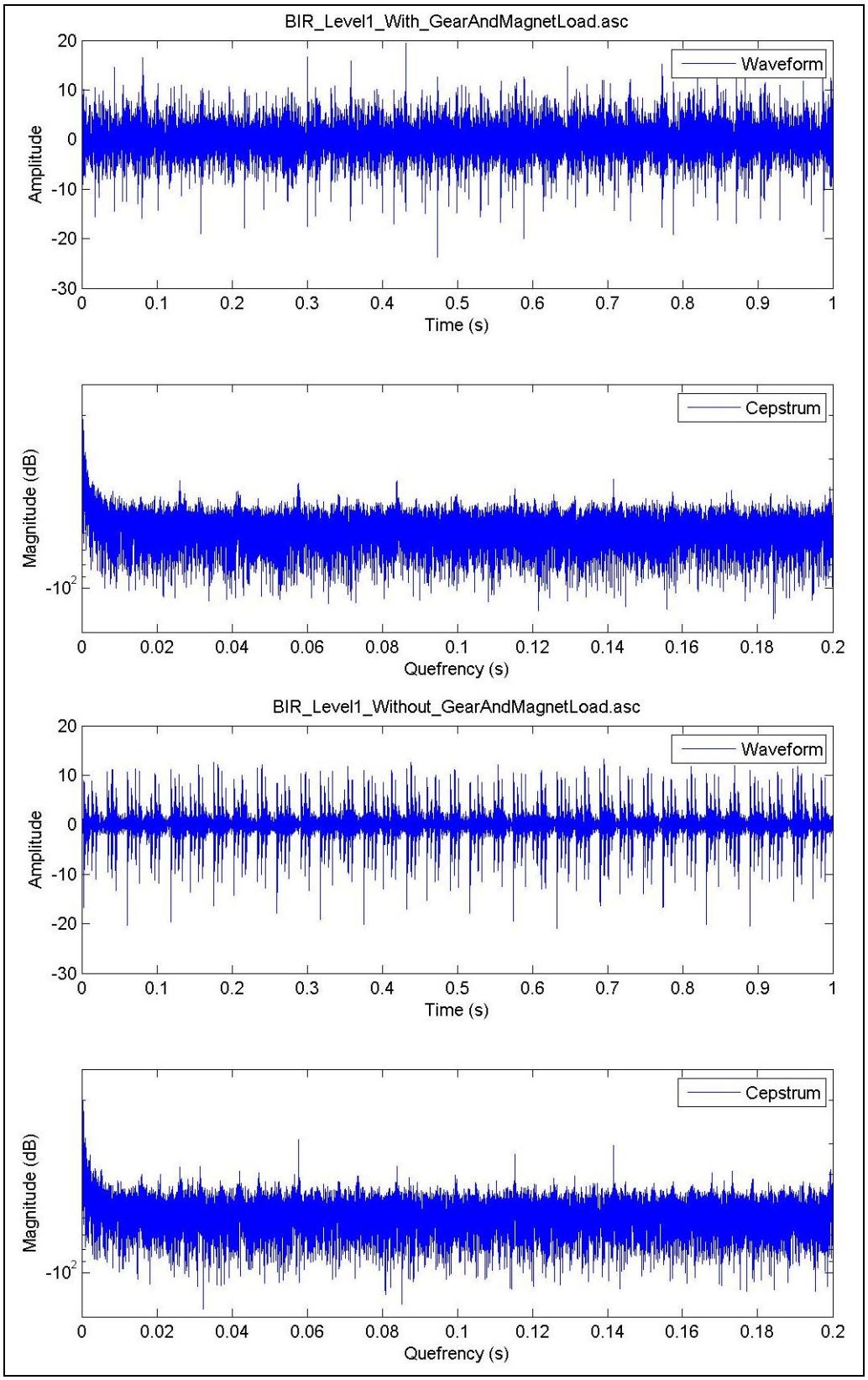

Figure B-4. Cepstrum algorithm for the inner race seeded fault bearings with and without gearbox and magnet load for level 1.

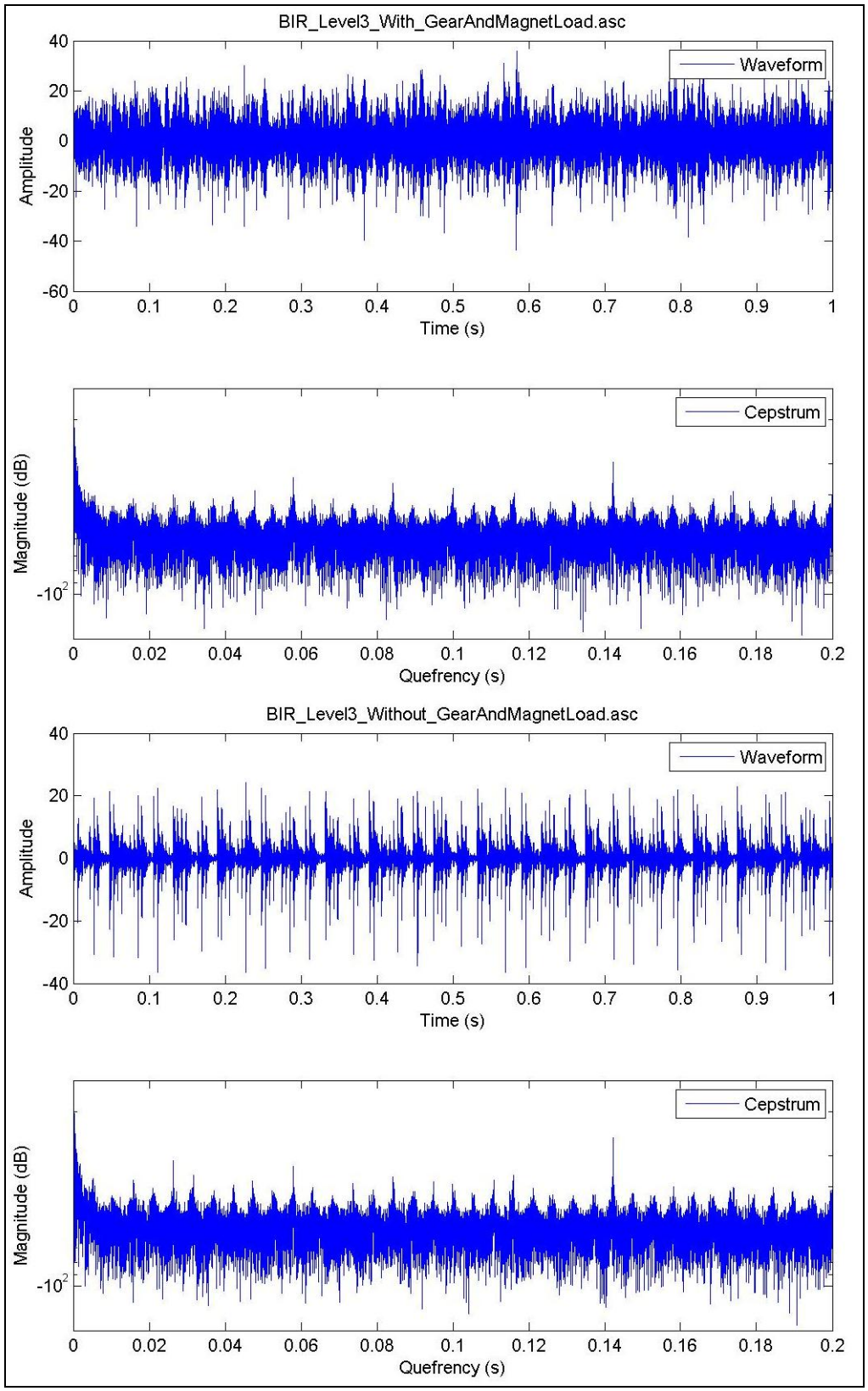

Figure B-5. Cepstrum algorithm for the inner race seeded fault bearings with and without gearbox and magnet load for level 3.

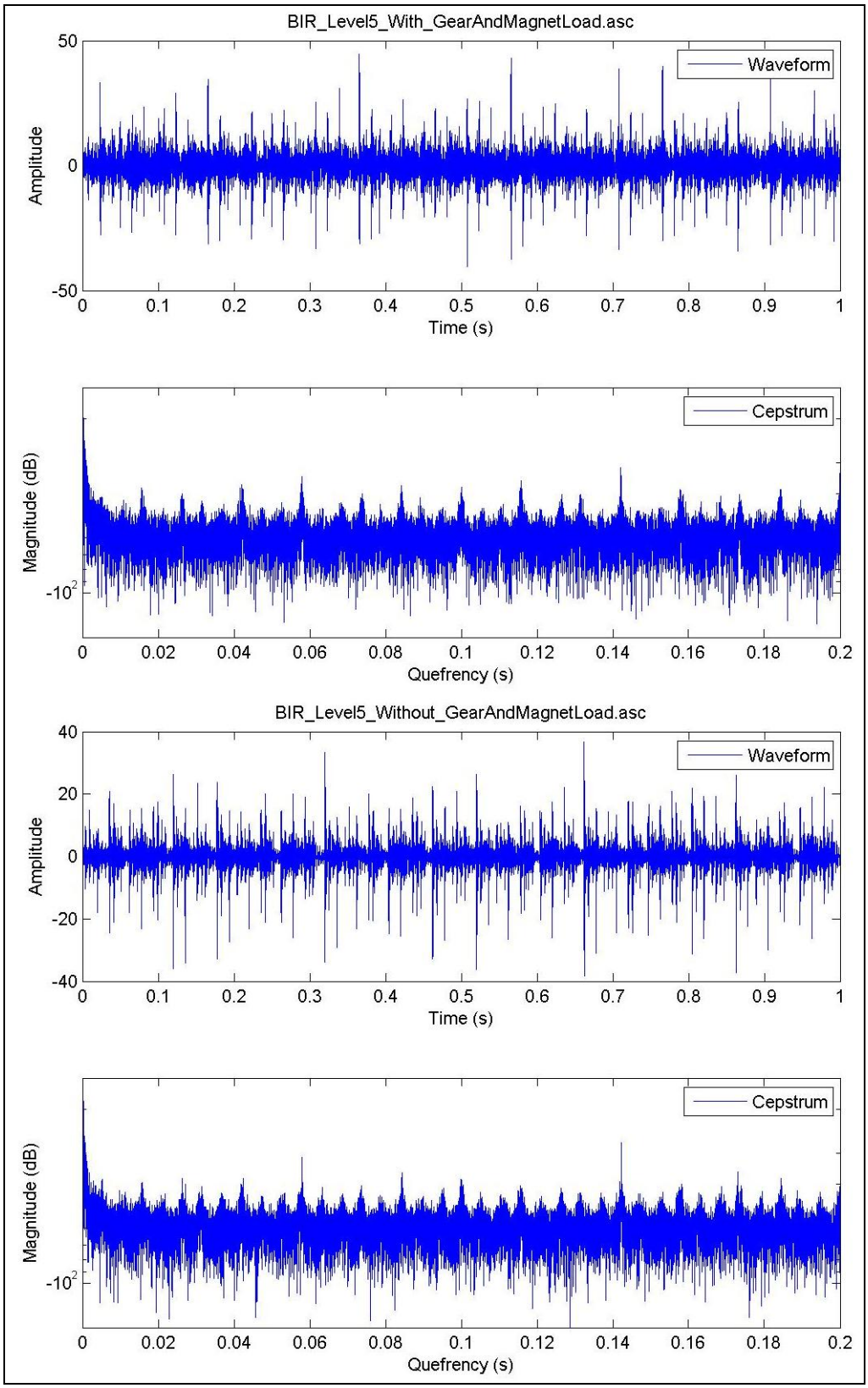

Figure B-6. Cepstrum algorithm for the inner race seeded fault bearings with and without gearbox and magnet load for level 5.

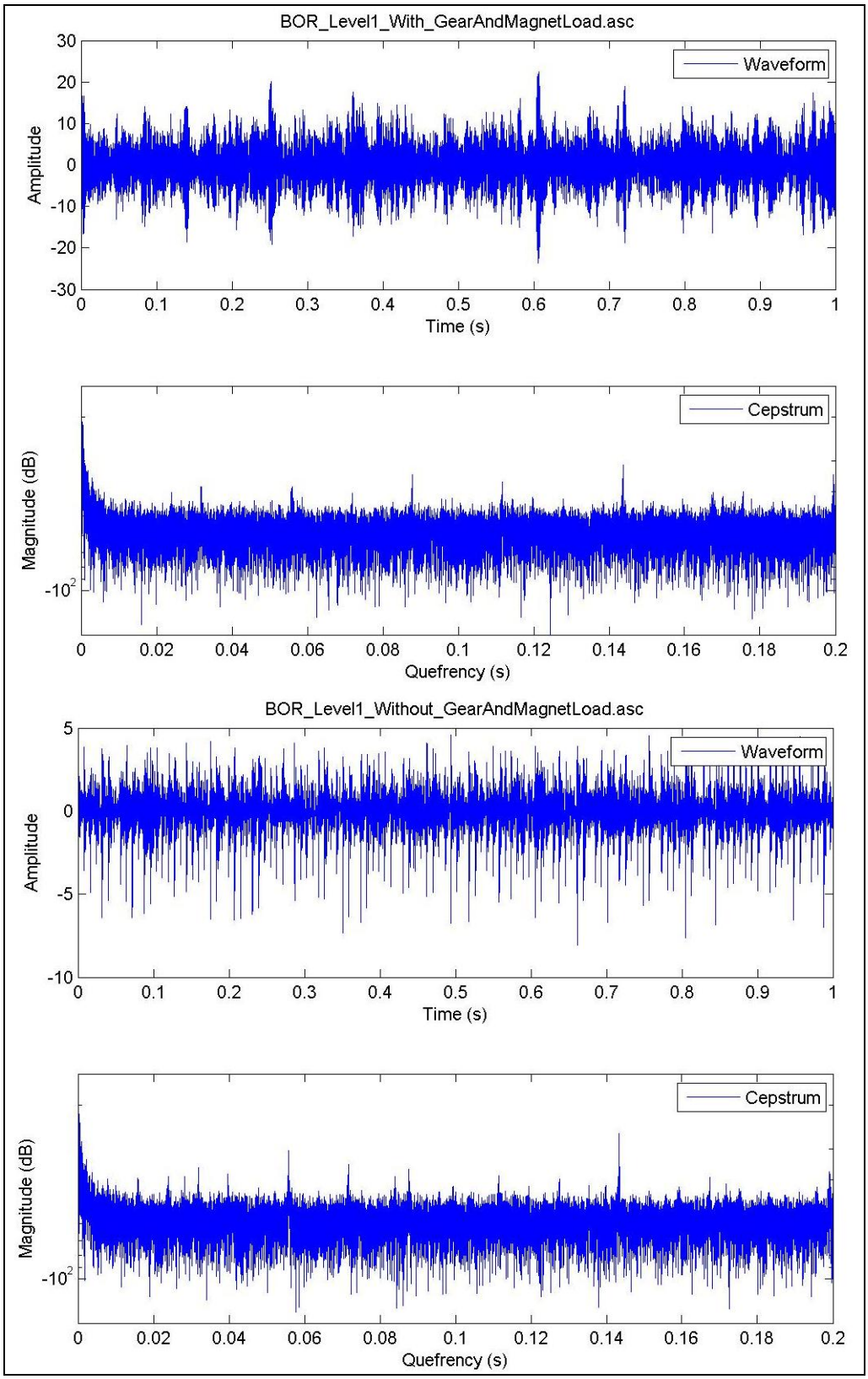

Figure B-7. Cepstrum algorithm for the outer race seeded fault bearings with and without gearbox and magnet load for level 1.

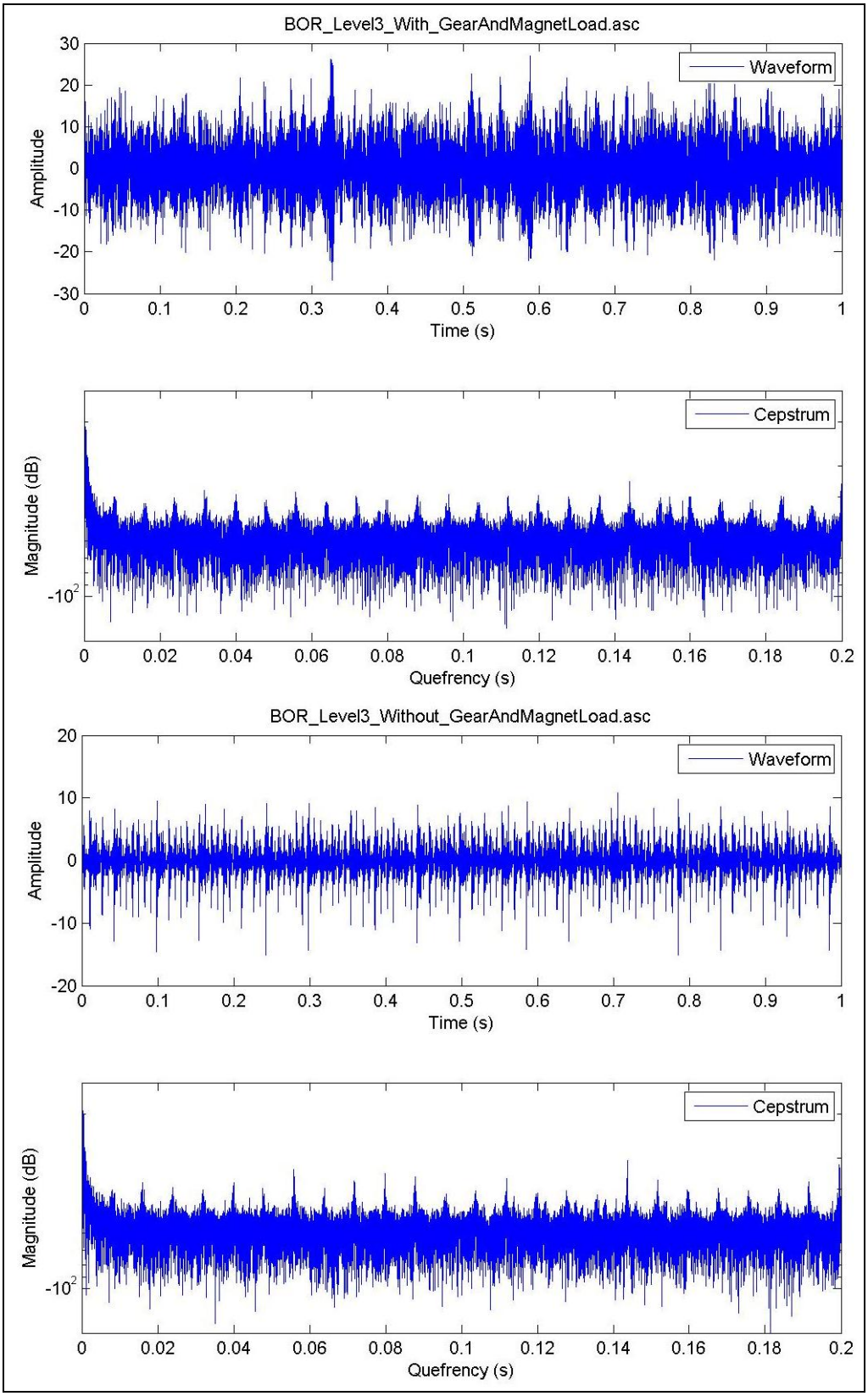

Figure B-8. Cepstrum algorithm for the outer race seeded fault bearings with and without gearbox and magnet load for level 3.

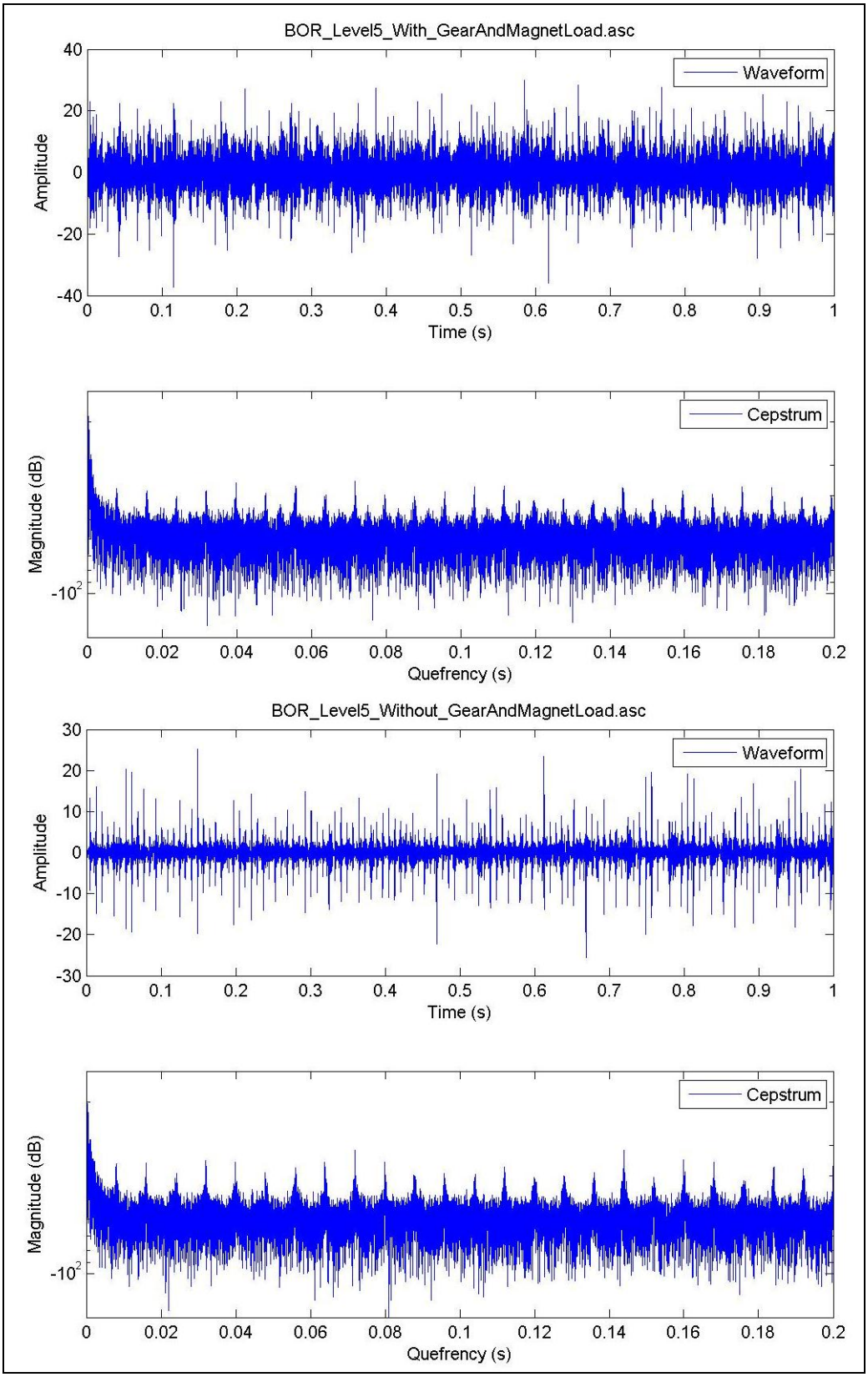

Figure B-9. Cepstrum algorithm for the outer race seeded fault bearings with and without gearbox and magnet load for level 5.

Appendix C. Results of the Cepstrum Algorithm for Selected Impact Data – Test 43, Bearing 2-2

This section consists of 24 graphs (12 for the axial direction and 12 for the radial direction). Two graphs show the result of the cepstrum for an Impact baseline data file. Other 22 graphs show the results of the cepstrum algorithm for the selected Impact Technologies' progressive seeded fault bearing, Test 43, Bearing 2-2.

C-1 Cepstrum for an Impact Baseline Data File

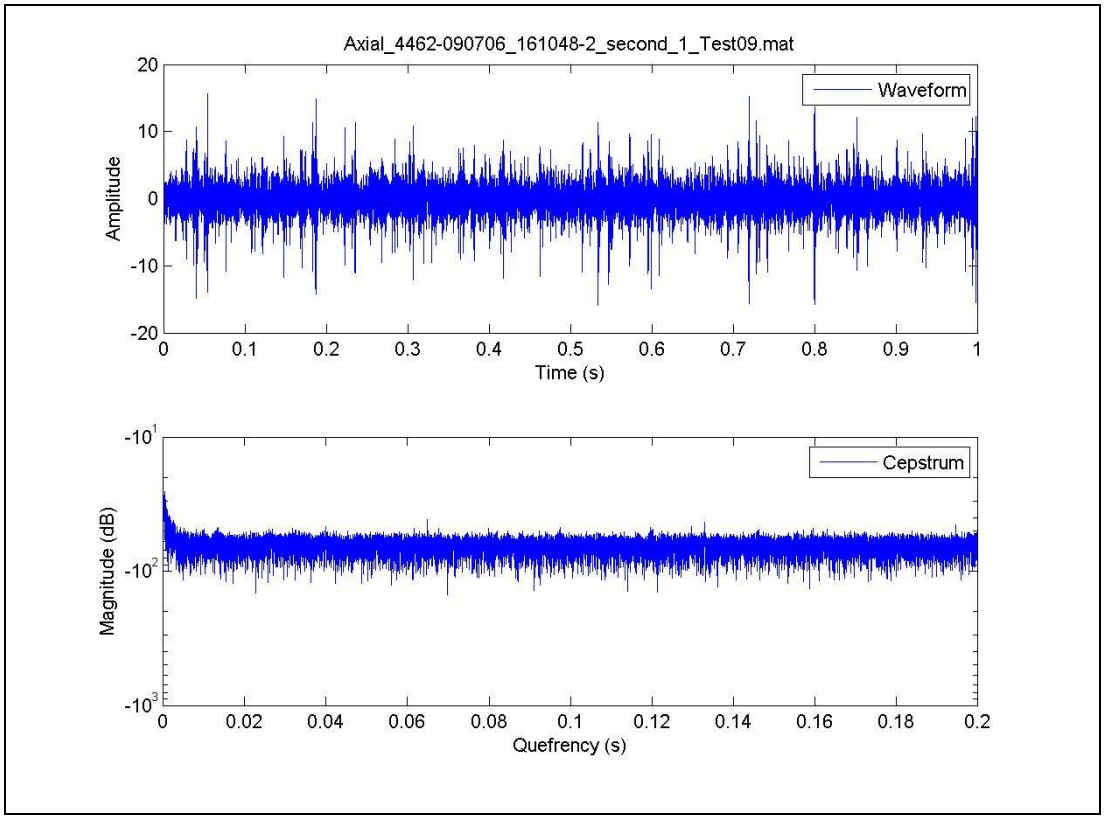

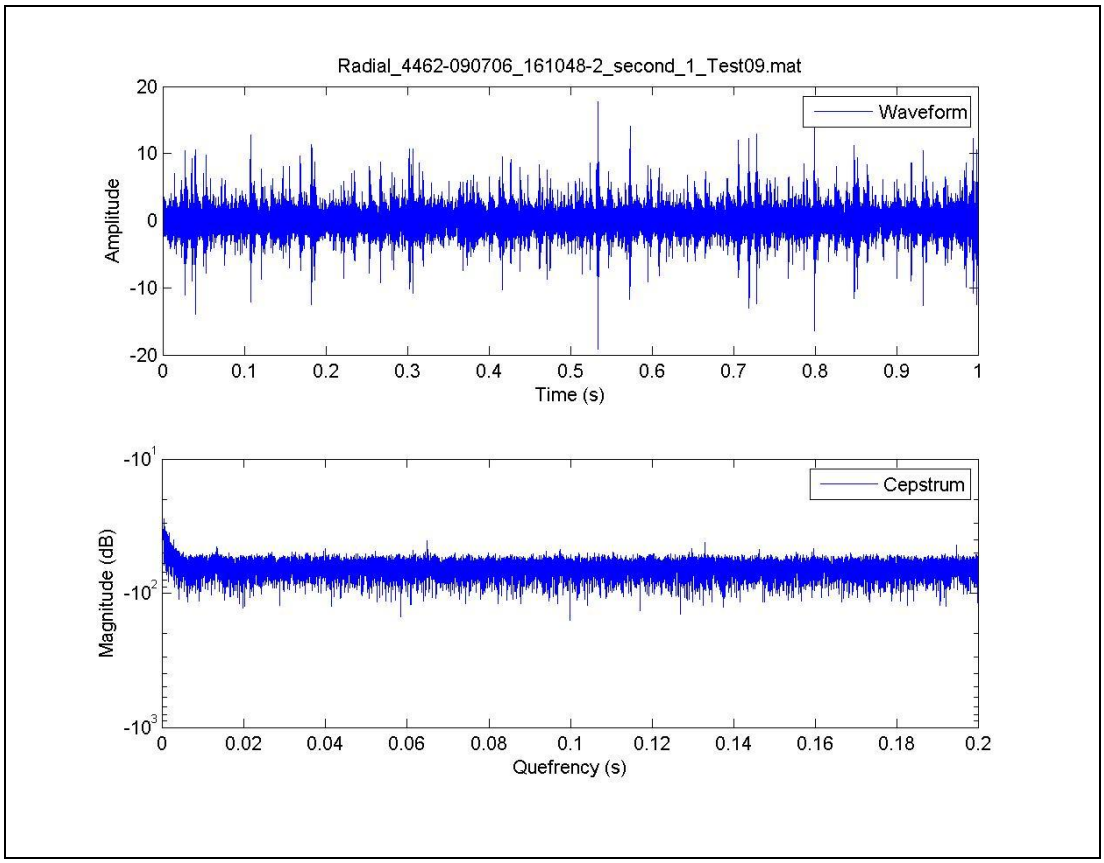

C-2 Cepstrum Algorithm for the Selected Impact Technologies' Progressive Seeded Fault Bearing, Test 43, Bearing 2-2

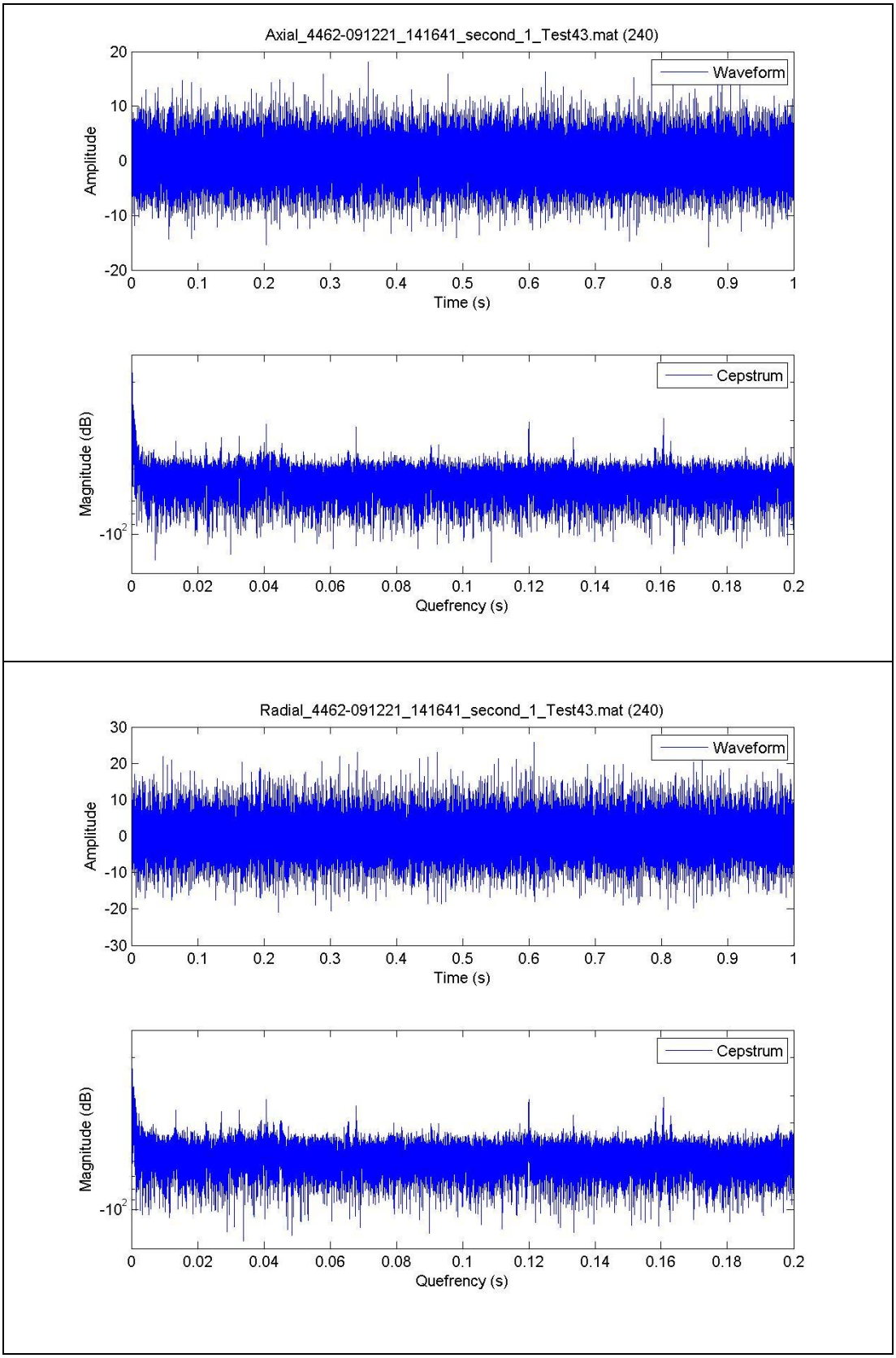
Axial_4462-091221_141641_second_1_Test43.mat (240)
Waveform
Amplitude
Time (s)
Cepstrum
Magnitude (dB)
Quefrency (s)
Radial_4462-091221_141641_second_1_Test43.mat (240)
Waveform
Amplitude
Time (s)
Cepstrum
Magnitude (dB)
Quefrency (s)

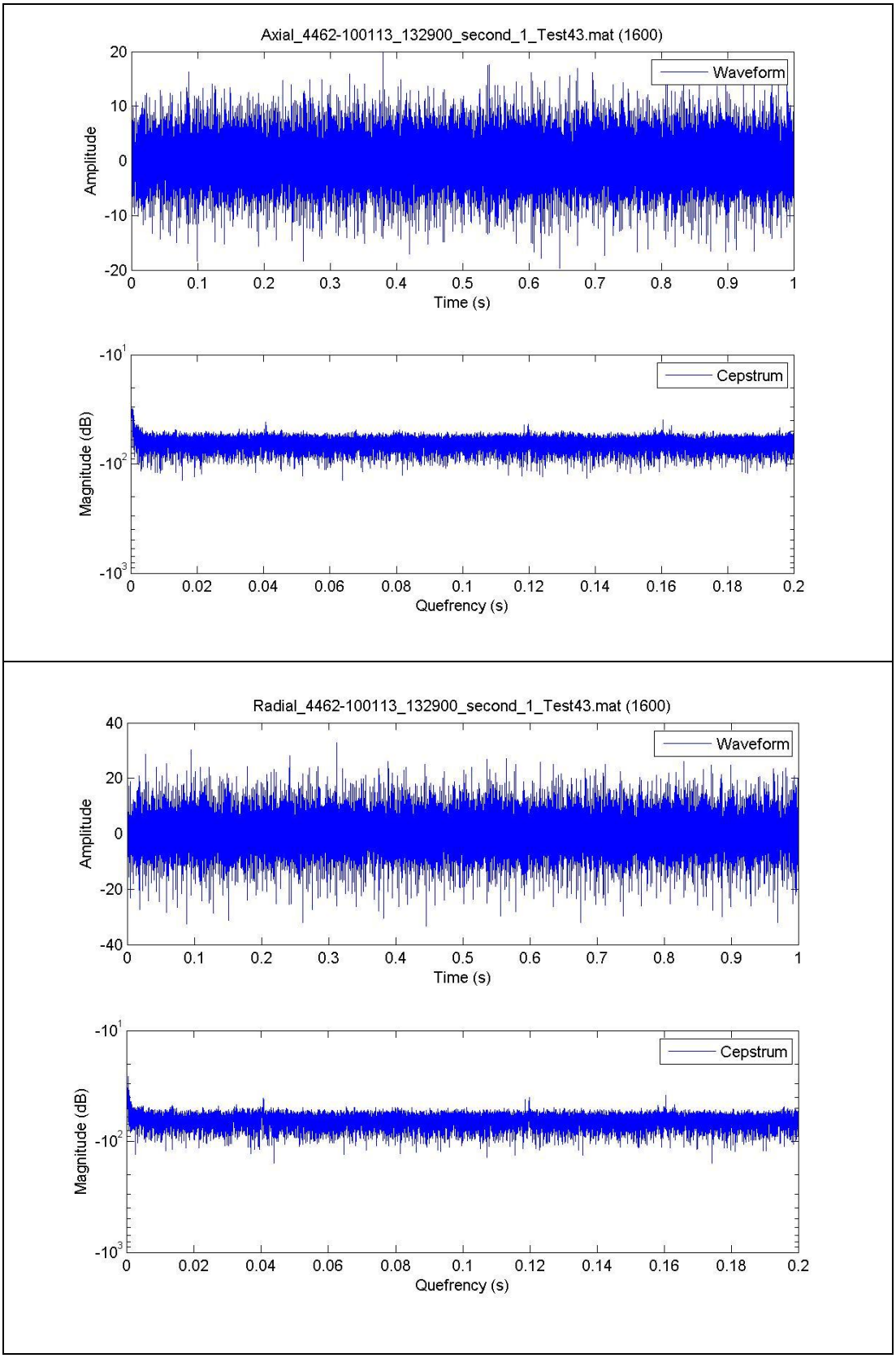
Axial_4462-100113_132900_second_1_Test43.mat (1600)
Waveform
Amplitude
Time (s)
Cepstrum
Magnitude (dB)
Quefrency (s)
Radial_4462-100113_132900_second_1_Test43.mat (1600)
Waveform
Amplitude
Time (s)
Cepstrum
Magnitude (dB)
Quefrency (s)

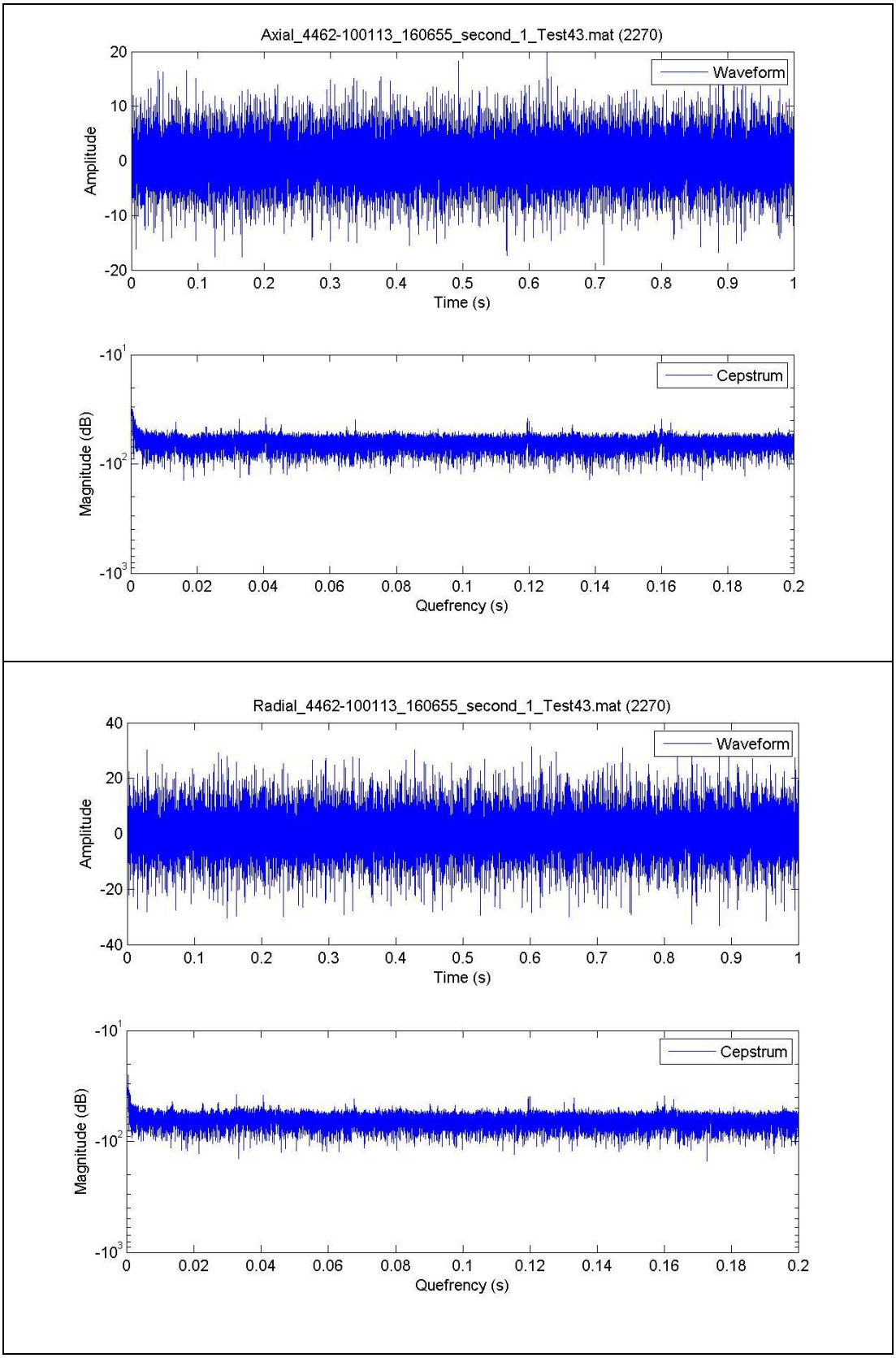
Axial_4462-100113_160655_second_1_Test43.mat (2270)
Waveform
Amplitude
Time (s)
Cepstrum
Magnitude (dB)
Quefrency (s)
Radial_4462-100113_160655_second_1_Test43.mat (2270)
Waveform
Amplitude
Time (s)
Cepstrum
Magnitude (dB)
Quefrency (s)

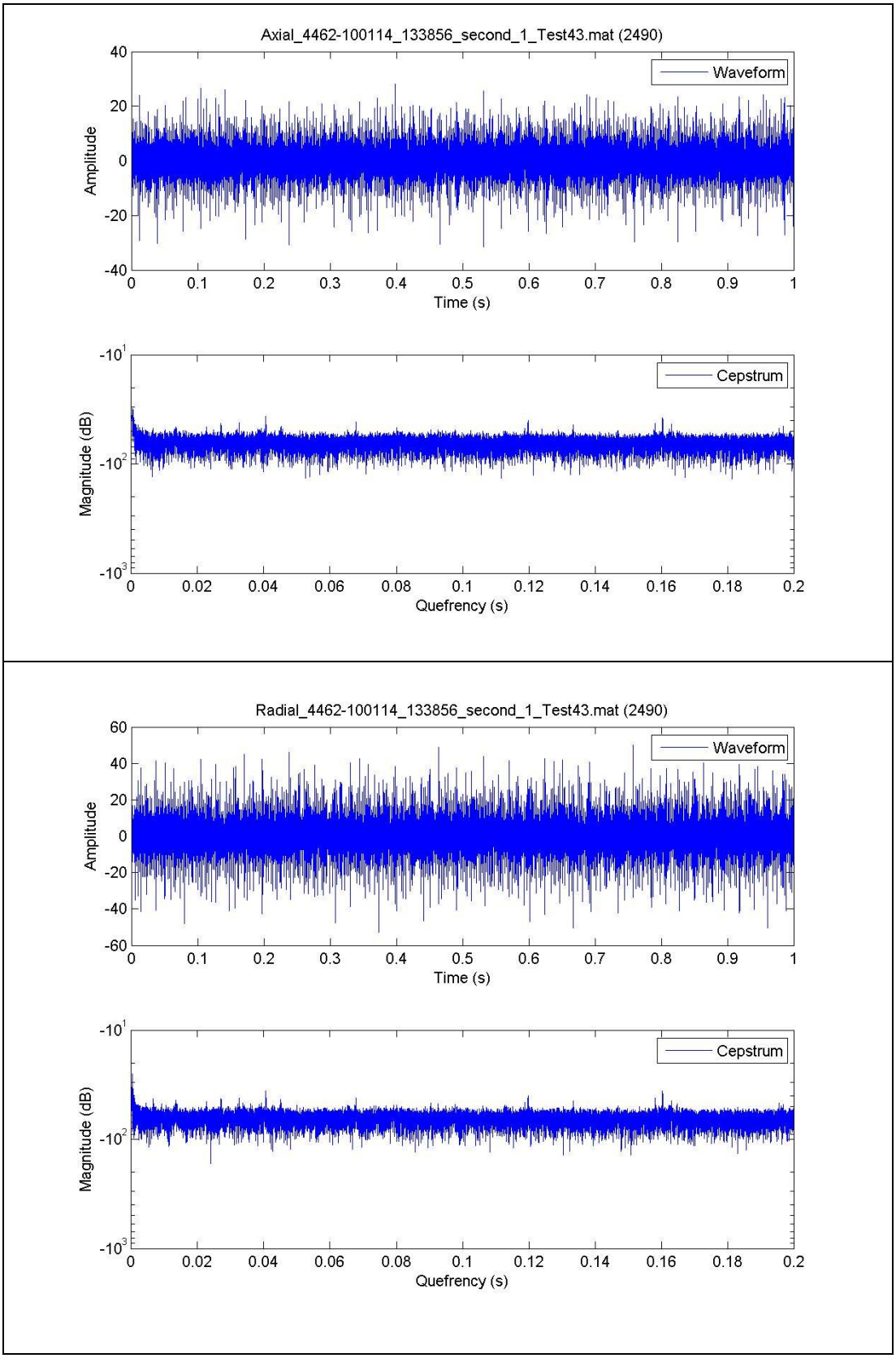
Axial_4462-100114_133856_second_1_Test43.mat (2490)
Waveform
Amplitude
Time (s)
Cepstrum
Magnitude (dB)
Quefrency (s)
Radial_4462-100114_133856_second_1_Test43.mat (2490)
Waveform
Amplitude
Time (s)
Cepstrum
Magnitude (dB)
Quefrency (s)

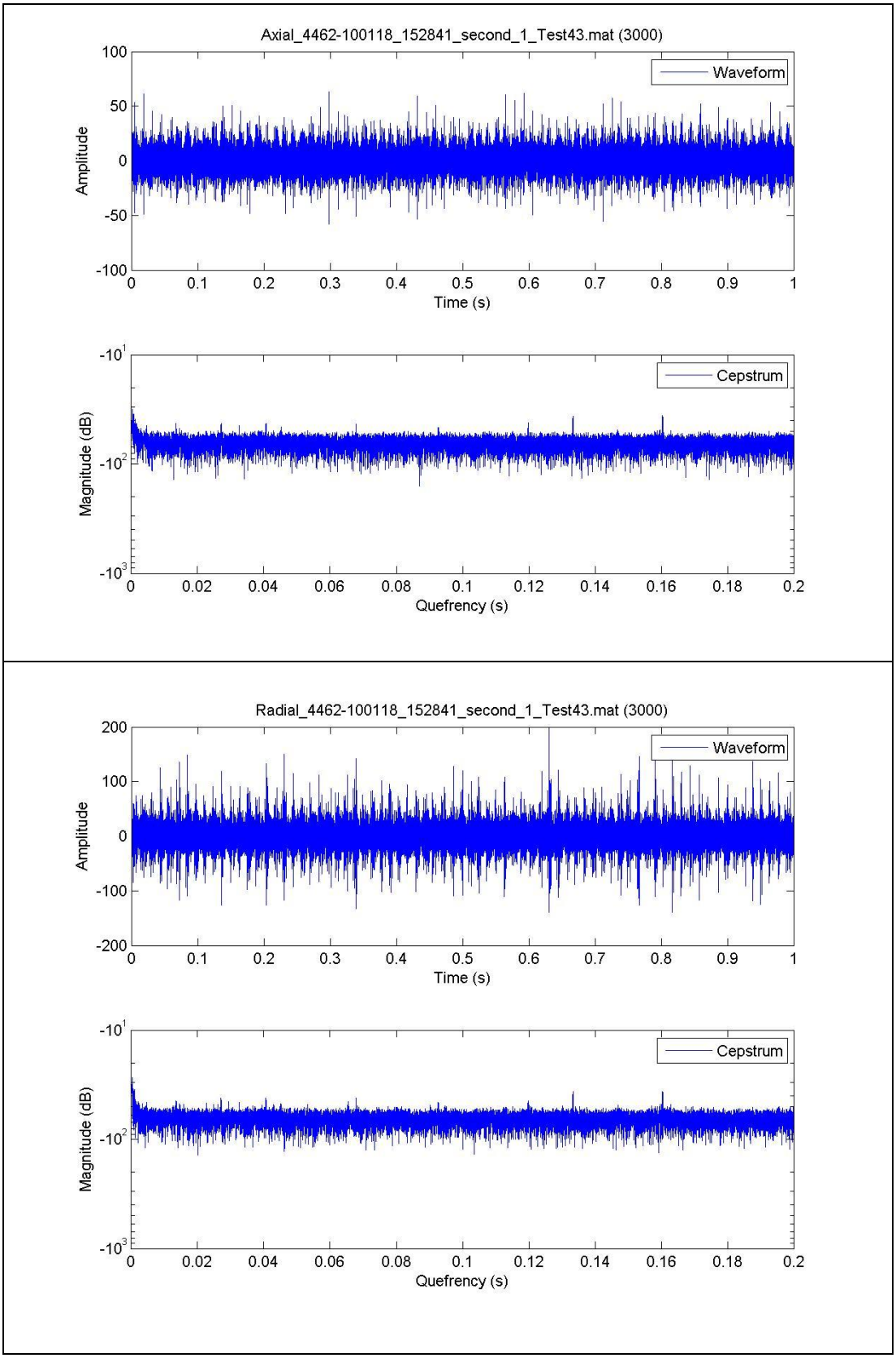
Axial_4462-100118_152841_second_1_Test43.mat (3000)
Waveform
Amplitude
Time (s)
Cepstrum
Magnitude (dB)
Quefrency (s)
Radial_4462-100118_152841_second_1_Test43.mat (3000)
Waveform
Amplitude
Time (s)
Cepstrum
Magnitude (dB)
Quefrency (s)

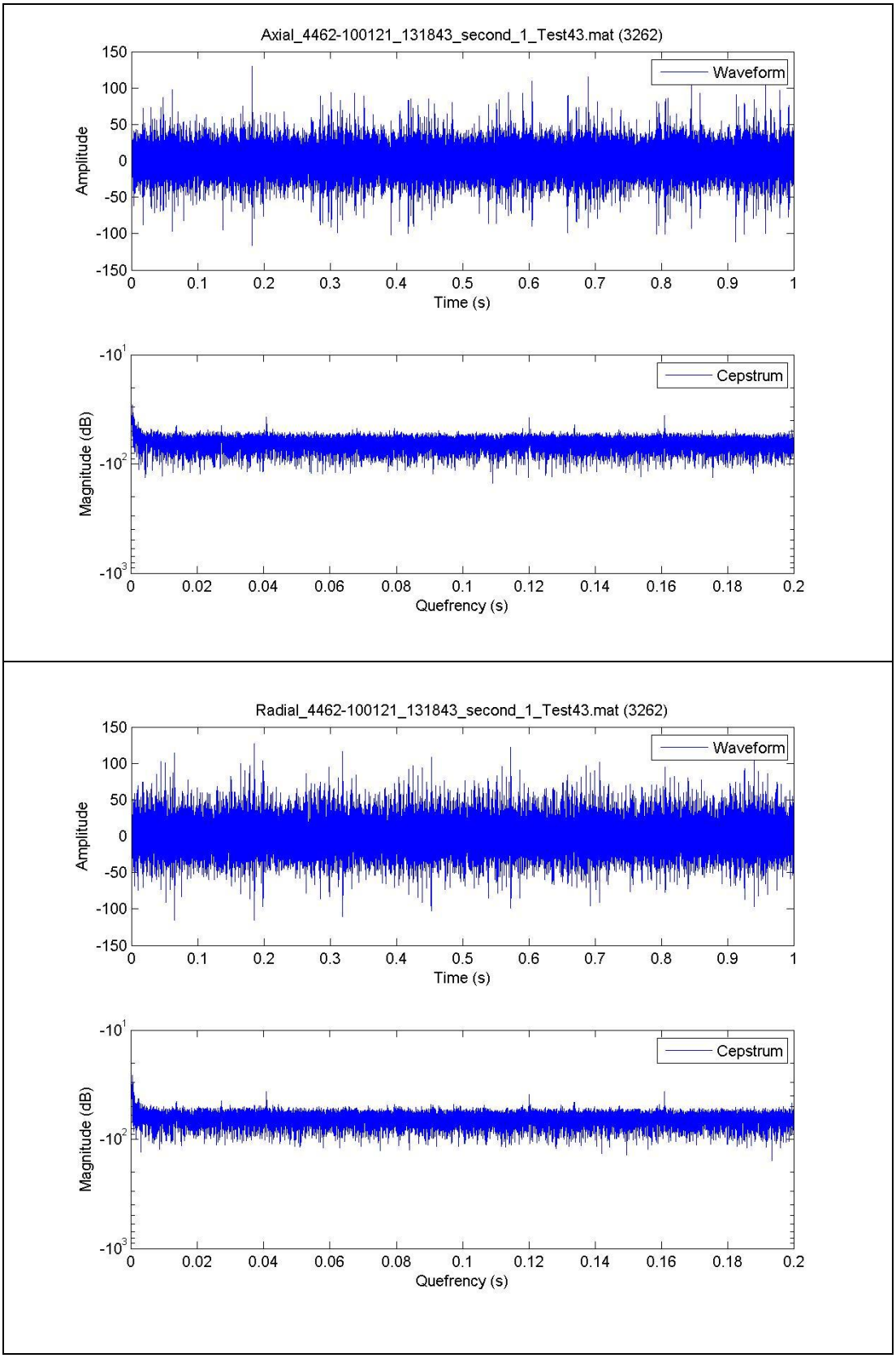
Axial_4462-100121_131843_second_1_Test43.mat (3262)
Waveform
Amplitude
Time (s)
Cepstrum
Magnitude (dB)
Quefrency (s)
Radial_4462-100121_131843_second_1_Test43.mat (3262)
Waveform
Amplitude
Time (s)
Cepstrum
Magnitude (dB)
Quefrency (s)

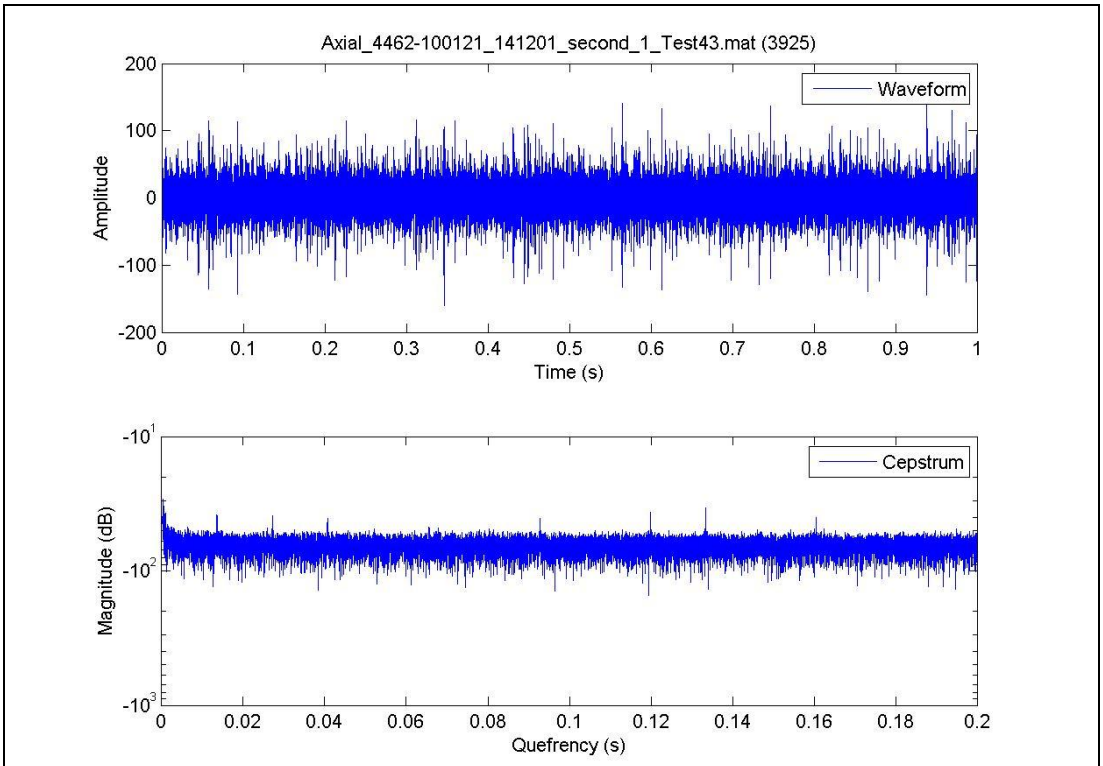
Axial_4462-100121_141201_second_1_Test43.mat (3925)
Waveform
Amplitude
Time (s)
Cepstrum
Magnitude (dB)
Quefrency (s)

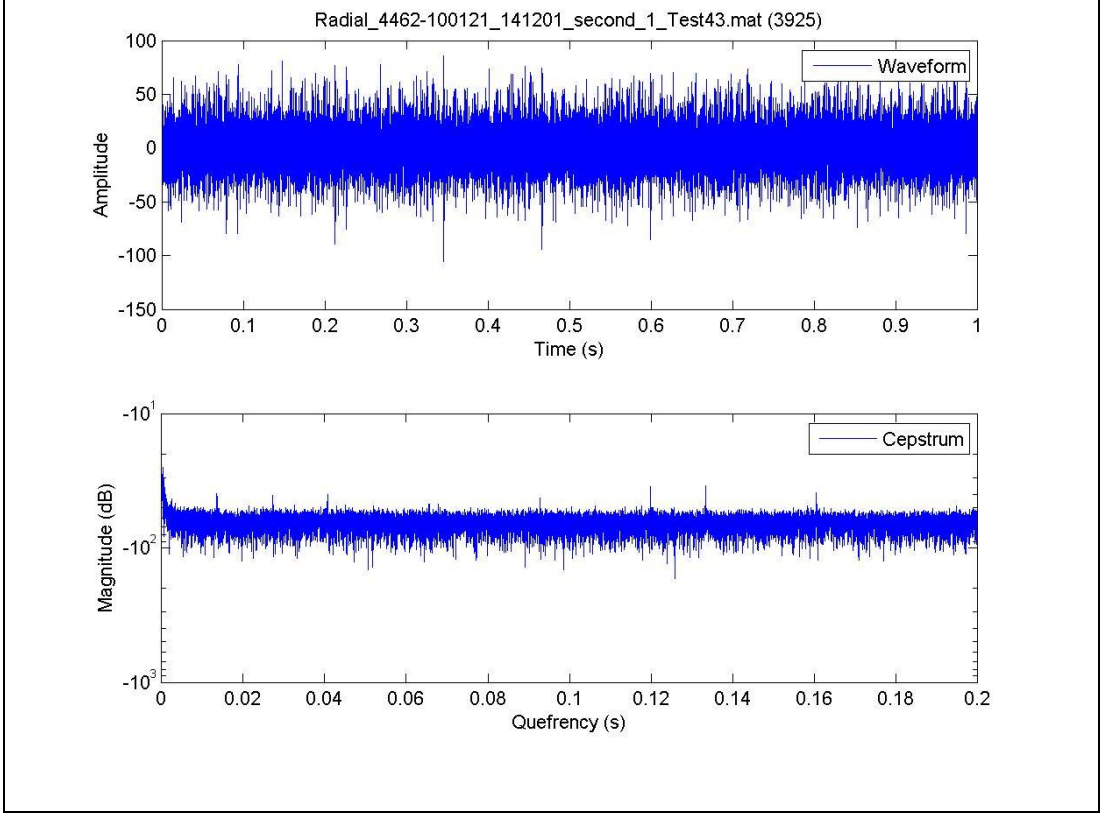
Radial_4462-100121_141201_second_1_Test43.mat (3925)
Waveform
Amplitude
Time (s)
Cepstrum
Magnitude (dB)
Quefrency (s)

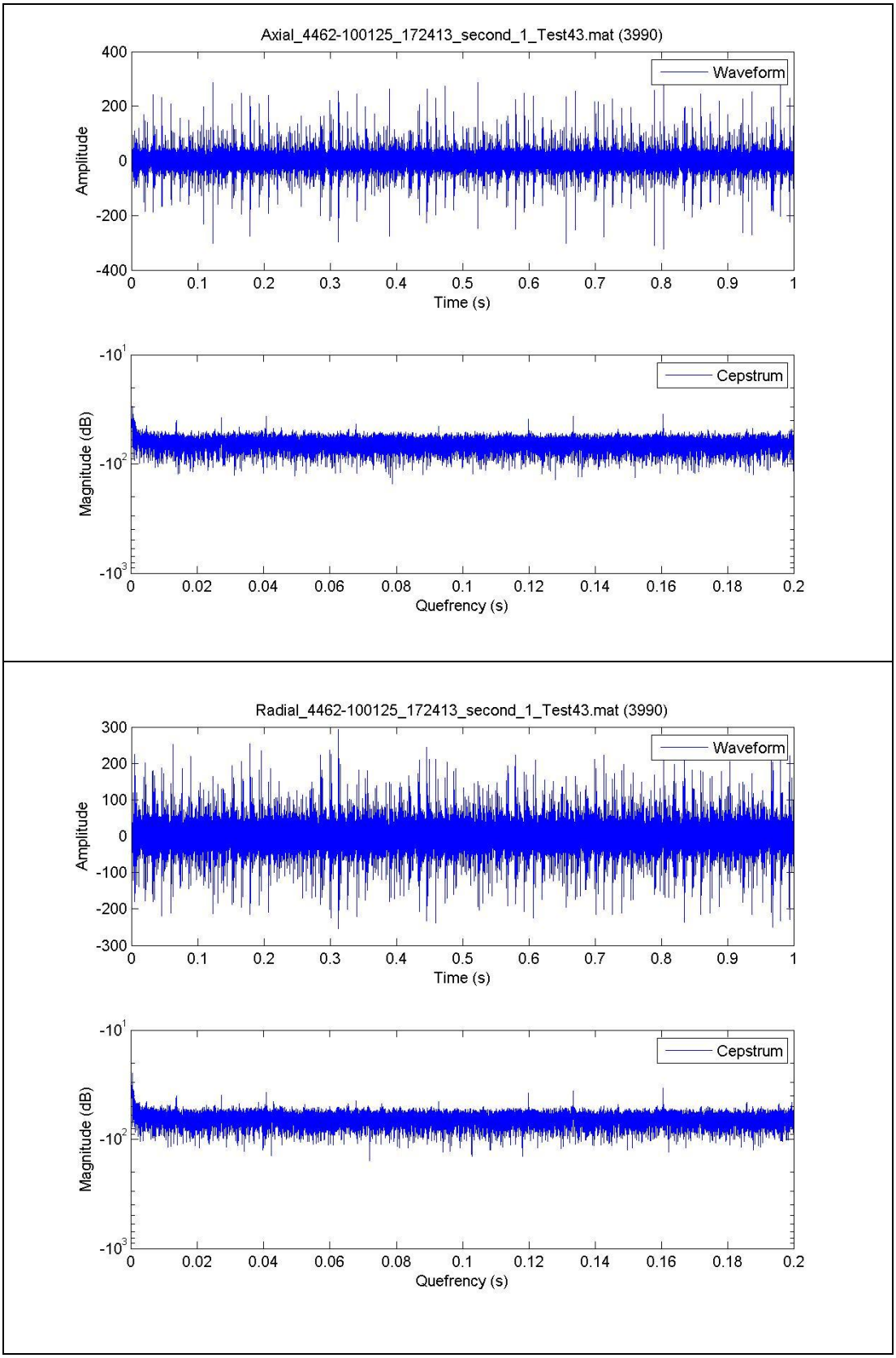
Axial_4462-100125_172413_second_1_Test43.mat (3990)
Waveform
Amplitude
Time (s)
Cepstrum
Magnitude (dB)
Quefrency (s)
Radial_4462-100125_172413_second_1_Test43.mat (3990)
Waveform
Amplitude
Time (s)
Cepstrum
Magnitude (dB)
Quefrency (s)

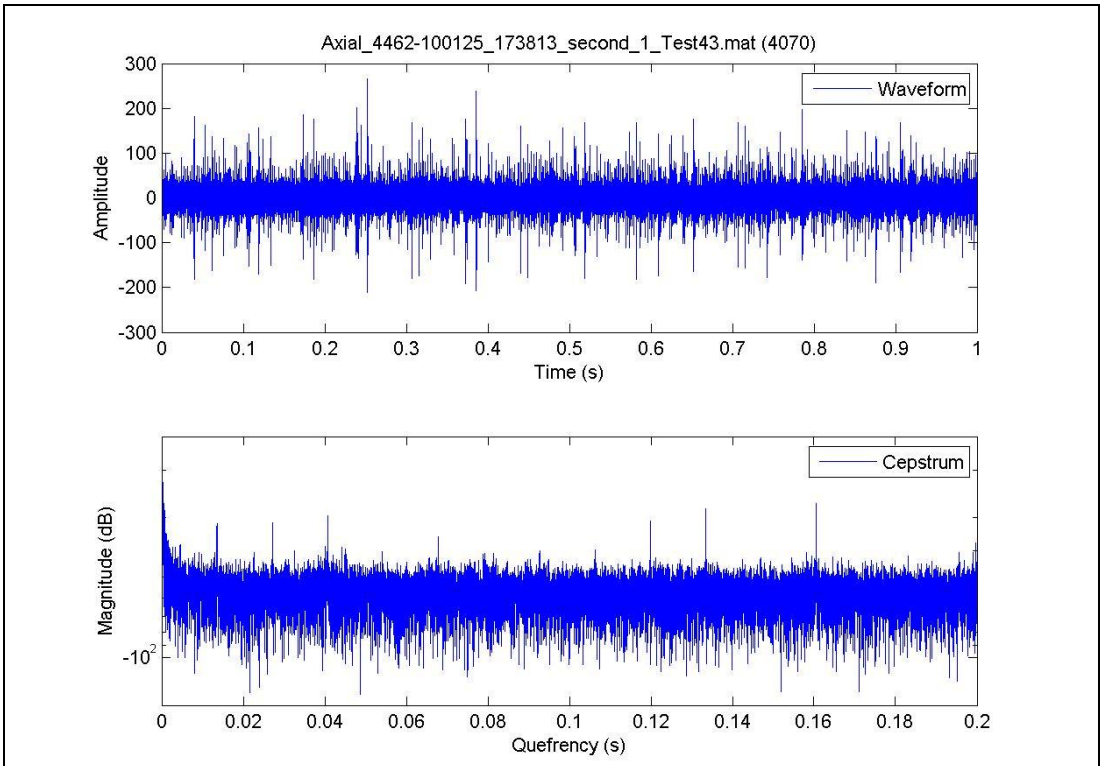
Axial_4462-100125_173813_second_1_Test43.mat (4070)
Waveform
Amplitude
Time (s)
Cepstrum
Magnitude (dB)
Quefrency (s)

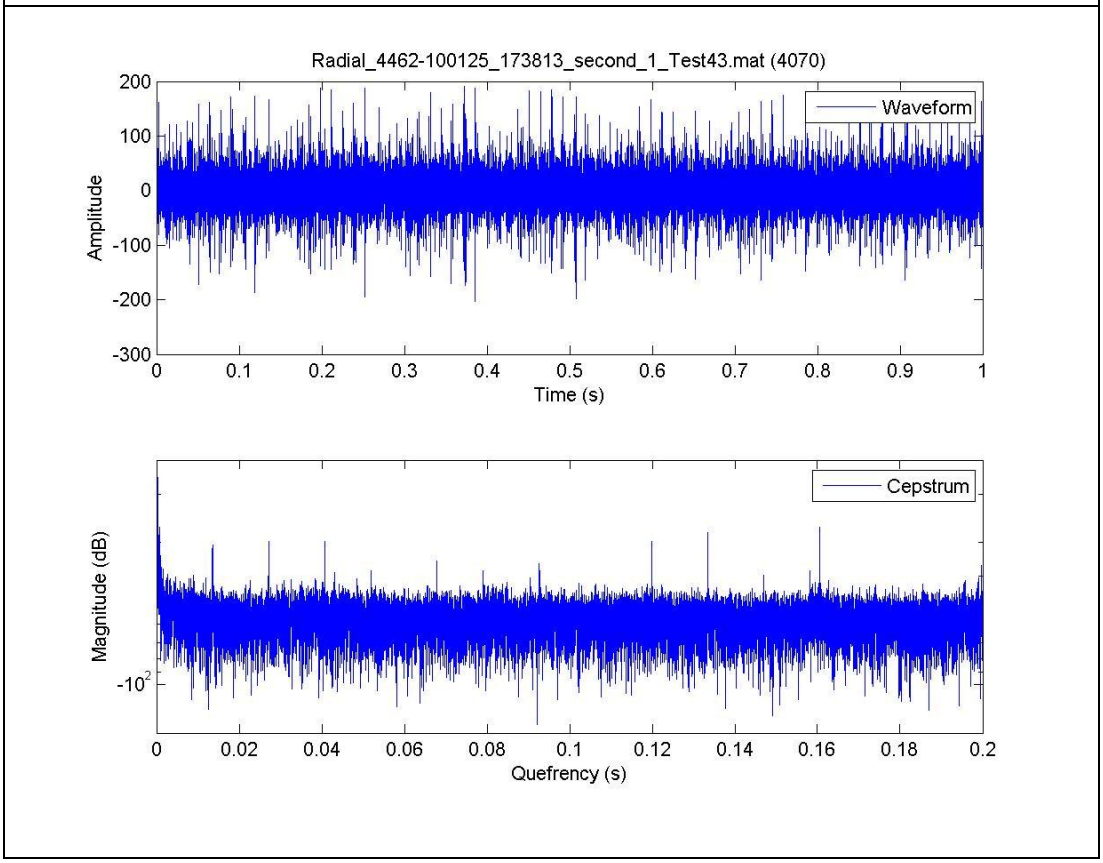
Radial_4462-100125_173813_second_1_Test43.mat (4070)
Waveform
Amplitude
Time (s)
Cepstrum
Magnitude (dB)
Quefrency (s)

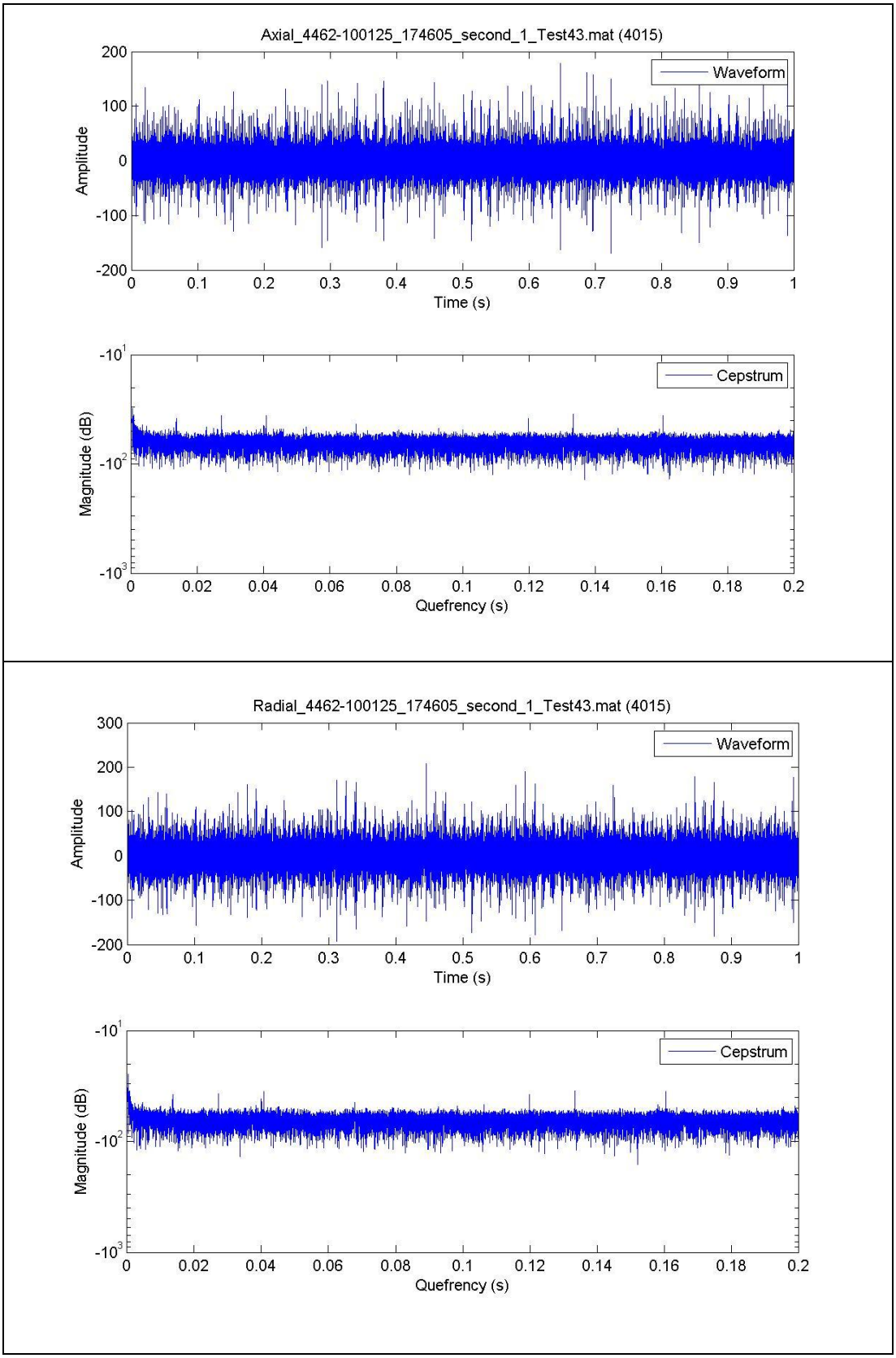
Axial_4462-100125_174605_second_1_Test43.mat (4015)
Waveform
Amplitude
Time (s)
Cepstrum
Magnitude (dB)
Quefrency (s)
Radial_4462-100125_174605_second_1_Test43.mat (4015)
Waveform
Amplitude
Time (s)
Cepstrum
Magnitude (dB)
Quefrency (s)

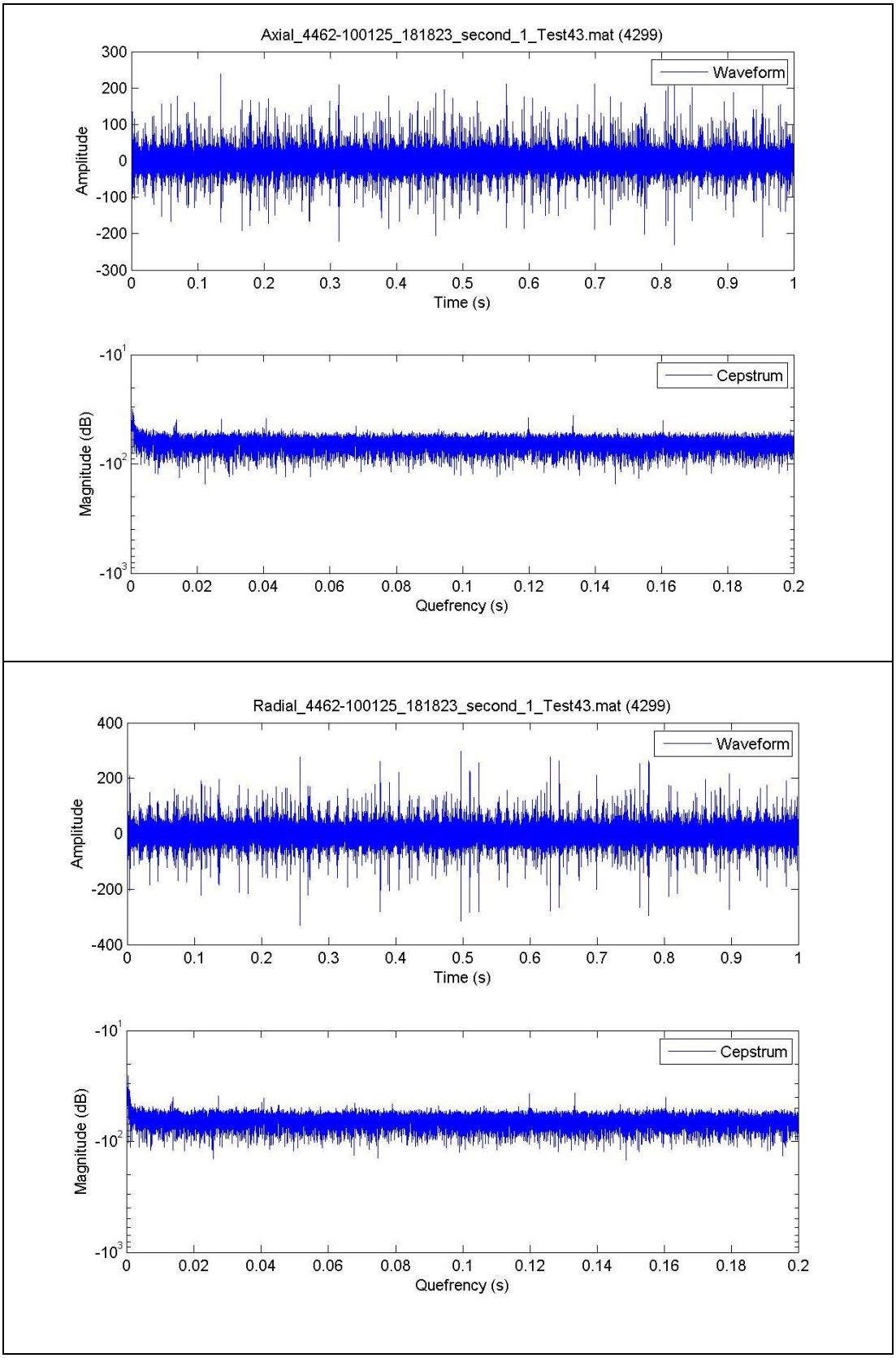
Axial_4462-100125_181823_second_1_Test43.mat (4299)
Waveform
Amplitude
Time (s)
Cepstrum
Magnitude (dB)
Quefrency (s)
Radial_4462-100125_181823_second_1_Test43.mat (4299)
Waveform
Amplitude
Time (s)
Cepstrum
Magnitude (dB)
Quefrency (s)

List of Symbols, Abbreviations, and Acronyms

ARL	U.S. Army Research Laboratory
BPFI	ball pass frequency inner race
BPFO	ball pass frequency outer race
BSF	ball spin frequency
FFT	fast Fourier transform
FTF	fault train frequency
MFS	Machine Fault Simulator
OEM	Original Equipment Manufacturer
SNR	signal-to-noise ratio

1 (PDF ONLY) DEFENSE TECHNICAL INFORMATION CTR
DTIC OCA
8725 JOHN J KINGMAN RD
STE 0944
FORT BELVOIR VA 22060-6218

1 DIRECTOR
US ARMY RESEARCH LAB
IMAL HRA
2800 POWDER MILL RD
ADELPHI MD 20783-1197

1 DIRECTOR
US ARMY RESEARCH LAB
RDRL CIO LL
2800 POWDER MILL RD
ADELPHI MD 20783-1197

5 DIRECTOR
US ARMY RESEARCH LAB
ATTN RDRL SER E
CANH LY
ROMEO DEL ROSARIO
KWOK TOM
ANDREW BAYBA
DERWIN WASHINGTON
ADELPHI MD 20783-1197

4 DIRECTOR
US ARMY RESEARCH LAB
ATTN RDRL VTM
DY LE
ANINDYA GHOSHAL
JAMES T. AYERS
MULUGETA HAILE
BUILDING 4603
APG MD 21005

INTENTIONALLY LEFT BLANK.